Organometallics 1988, 7, 106-117

Chemical Transformations on Phosphido-Bridged Clusters. Synthesis of the 48- and 50-Electron Acetylide Complexes $Ru_3(CO)_n\{\mu_3\text{-}\eta^2\text{-}C{\equiv}C(i\text{-}Pr)\}(\mu\text{-}PPh_2)$ (n = 8, 9) and Their Reactions with Diazomethane. Carbon–Carbon Bond Forming Reactions and the Conversion of Acetylide to Allenyl Clusters

D. Nucciarone, S. A. MacLaughlin, N. J. Taylor, and A. J. Carty*

Guelph-Waterloo Centre for Graduate Work in Chemistry, Department of Chemistry, University of Waterloo, Waterloo, Ontario, Canada N2L 3G1

Received April 8, 1987

The 50-electron phosphido-bridged clusters $Ru_3(CO)_9\{\mu_3\text{-}\eta^2\text{-}C{\equiv}CR\}(\mu\text{-}PPh_2)$ (R = *i*-Pr, **2a**; R = *t*-Bu, **2b**) have been synthesized from $Ru_3(CO)_{11}(Ph_2PC{\equiv}CR)$ (**1a**,**b**) via controlled oxidative insertion into the P–C bond of the phosphinoalkyne. These compounds lose CO at 60 °C affording the 48-electron clusters $Ru_3(CO)_6(\mu\text{-}CO)_2\{\mu_3\text{-}\eta^2\text{-}C{\equiv}CR\}(\mu\text{-}PPh_2)$ (R = *i*-Pr, **3a**; R = *t*-Bu, **3b**). Full single-crystal X-ray structural analyses of **2a** and **3b** have been carried out. Compound **2a** crystallizes in the monoclinic space group $P2_1/c$ with a = 13.189 (1) Å, b = 9.674 (1) Å, c = 22.481 (2) Å, β = 91.82 (1)°, and Z = 4. The structure was refined to R and R_w values of 0.025 and 0.028 with use of 2743 observed (3785 measured) reflections. The molecule has an open triangular structure with two strong Ru–Ru interactions and an axial μ-PPh_2 group bridging the long (Ru(1)–Ru(3) = 3.4658 (6) Å) edge. The 48-electron decarbonylation product **3b** crystallizes in a triclinic cell, space group $P\bar{1}$, with a = 9.674 (1) Å, b = 13.373 (1) Å, c = 13.654 (1) Å, α = 108.97 (1)°, β = 72.64 (1)°, γ = 93.79 (2)°, and Z = 2. Final R and R_w values based on 4911 observed diffractometer data were 0.029 and 0.031. Principal structural features are an equatorial phosphido bridge across a short Ru–Ru bond (Ru(1)–Ru(3) = 2.8257 (4) Å), two bridging carbonyls across the other edges of the Ru_3 triangle, and a μ_3-η^2-acetylide on the Ru_3 face. Reactions of **2a** and **3a** with CH_2N_2 have been explored. The cluster **3a** reacts rapidly with diazomethane affording the μ_3-allenyl cluster $Ru_3(CO)_8\{\mu_3\text{-}\eta^3\text{-}CH_2{=}C{=}C(i\text{-}Pr)\}(\mu\text{-}PPh_2)$ (**4**) via coupling of a methylene (CH_2) unit with the acetylide. Isolation of **4** and further reaction with CH_2N_2 gave the μ-methylene cluster $Ru_3(CO)_7(\mu\text{-}CH_2)\{\mu_3\text{-}\eta^3\text{-}CH_2{=}C{=}C(i\text{-}Pr)\}(\mu\text{-}PPh_2)$ (**5**). Both **4** and **5** have been fully characterized by single-crystal X-ray diffractometry. Complex **4** crystallizes in space group $P2_1/c$ with a = 11.892 (2) Å, b = 12.200 (2) Å, c = 19.698 (4) Å, β = 93.22 (1)°, and Z = 4. Crystals of **5** are monoclinic space group $P2_1/c$ with a = 11.890 (2) Å, b = 11.973 (1) Å, c = 19.675 (2) Å, β = 90.10 (1)°, and Z = 4. Final R and R_w values were 0.029 and 0.031, respectively, for **4** and 0.035 and 0.039, respectively, for **5**. The clusters **4** and **5** are remarkably similar in skeletal stereochemistry with the allenyl fragments and the phosphido bridges being almost identically coordinated on the trinuclear framework. In **5** however a μ-CH_2 group bridges one Ru–Ru bond, replacing a CO ligand in **4**. The nature of the carbon–carbon bond forming reactions and the structural relationships between **2a**, **3b**, **4**, and **5** are discussed.

Over the last 12 years we have been systematically exploring the chemistry of phosphido bridged bi- and polynuclear compounds.[1] This area has recently witnessed a tremendous growth and the number of known phosphido-bridged complexes now lists in the thousands. A principal motivation for the recent upsurge in interest has been the hope that μ-PR_2 bridges might function as strongly bound, flexible but inert ligands, capable of maintaining the molecularity of a polymetallic framework under conditions where useful chemistry might be accomplished.[2] For binuclear systems a number of interesting and potentially useful transformations have been documented,[3] but there is both recent[4] and longstanding[5] evidence that the μ-PR_2 group may behave under certain conditions as a noninnocent ligand toward nucleophilic[6] and electrophilic[7] reagents. Clearly such reactivity is to be expected in the absence of other, more favorable reaction sites and pathways. The development of useful chemistry for phosphido complexes thus hinges on the presence of other, activated ligands susceptible to attack

---

(1) For reviews of our work in this area see: (a) Carty, A. J. *Adv. Chem. Ser.* **1982**, *No. 196*, 163. (b) Carty, A. J. *Pure Appl. Chem.* **1982**, *54*, 113. (c) Fehlhammer, W. P.; Stolzenberg, H. In *Comprehensive Organometallic Chemistry*; Wilkinson, G., Stone, F. G. A., Abel, E. W., Eds.; Pergamon: Oxford, 1982; Vol. 4, Chapter 31, pp 513–613. (d) Nast, R. *Coord. Chem. Rev.* **1982**, *47*, 89. (e) Carty, A. J.; MacLaughlin, S. A.; Nucciarone, D. In *Phosphorus-31 NMR Spectroscopy in Stereochemical Analysis: Organic Compounds and Metal Complexes*; Verkade, J. G., Quin, L. D., Eds.; VCH Publishers: New York, 1986; Chapter 16, pp 559–619.

(2) For a selection of recent references to phosphido bridged compounds see: (a) Targos, T. S.; Geoffroy, G. L.; Rheingold, A. *Organometallics* **1986**, *5*, 12. (b) Roddick, D. M.; Santasiero, B. D.; Bercaw, J. E. *J. Am. Chem. Soc.* **1985**, *107*, 4670. (c) Patel, V. D.; Cherkas, A. A.; Nucciarone, D.; Taylor, N. J.; Carty, A. J. *Organometallics* **1985**, *4*, 1792. (d) Kang, S. K.; Albright, T. A.; Wright, T. C.; Jones, R. A. *Organometallics* **1985**, *4*, 666. (e) Colbran, S. B.; Johnson, B. F. G.; Lewis, J.; Sorrel, S. M. *J. Organomet. Chem.* **1985**, *296*, C1. (f) Chen, L.; Kountz, D. J.; Meek, D. W. *Organometallics* **1985**, *4*, 598. (g) Werner, H.; Zolk, R. *Organometallics* **1985**, *4*, 601. (h) Powell, J.; Sawyer, J. F.; Smith, S. J. *J. Chem. Soc., Chem. Commun.* **1985**, 1312. (i) Yu, Y. F.; Galluci, J. C.; Wojcicki, A. *J. Chem. Soc., Chem. Commun.* **1984**, 653. (j) Henrick, K.; Iggo, K.; Mays, M. J.; Raithby, P. R. *J. Chem. Soc., Chem. Commun.* **1984**, 209. (k) Bender, R.; Braunstein, P.; Metz, B.; Lemoine, P. *Organometallics* **1984**, *3*, 381. (l) Deppisch, B.; Schafer, H.; Binder, D.; Leske, W. *Z. Anorg. Allg. Chem.* **1984**, *519*, 53. (m) McKennis, J. S.; Kyba, E. P. *Organometallics* **1983**, *2*, 1249. (n) Baker, R. T.; Tulip, T. H.; Wreford, S. S. *Inorg. Chem.* **1985**, *24*, 1379.

(3) See for example ref 2 and: (a) Collman, J. P.; Rothrock, R. K.; Finke, R. G.; Rose-Munch, F. *J. Am. Chem. Soc.* **1977**, *99*, 7381. (b) Mott, G. N.; Carty, A. J. *Inorg. Chem.* **1983**, *22*, 2786. (c) Breen, M. J.; Shulman, P. M.; Geoffroy, G. L.; Rheingold, A. L.; Fultz, W. C. *Organometallics* **1984**, *3*, 782. (d) Langenbach, H. J.; Keller, E.; Vahrenkamp, H. *Angew. Chem., Int. Ed. Engl.* **1977**, *16*, 188.

(4) A survey of the plethora of reactions observed for phosphido bridges is given in: Rosenberg, S.; Geoffroy, G. L.; Rheingold, A. L. *Organometallics* **1985**, *4*, 1184.

0276-7333/88/2307-0106$01.50/0

by nucleophilic or electrophilic reagents. We have shown that multisite-bound unsaturated ligands in binuclear phosphido-bridged complexes can be successfully derivatized with nucleophilic reagents, affording new C–C,[8] C–N,[9] C–P,[10] and C–S[11] bonds without destroying the μ-PR_2 bridge. Work in other laboratories has focussed mainly on reactions at the metal sites (e.g., oxidative addition of dihydrogen[3c]) rather than hydrocarbon elaboration.

Apart from studies on the reactivity of the cluster framework,[13] relatively little has been reported pertaining to reactions of unsaturated hydrocarbon ligands in phosphido-(or arsenido-) bridged clusters. In the first of this series of papers we describe the synthesis of the 48- and 50-electron phosphido-bridged acetylides $Ru_3(CO)_n\{\mu_3\text{-}\eta^2\text{-}C{\equiv}C(i\text{-}Pr)\}(\mu\text{-}PPh_2)$ (n = 8, 9), their characterization, and reactions with diazomethane leading, via C–C coupling, to the μ_3-allenyl complex $Ru_3(CO)_8\{\mu_3\text{-}\eta^3\text{-}CH_2{=}C{=}C(i\text{-}Pr)\}(\mu\text{-}PPh_2)$ and subsequently the μ-methylene cluster $Ru_3(CO)_7\{\mu_3\text{-}\eta^3\text{-}CH_2{=}C{=}C(i\text{-}Pr)\}(\mu\text{-}CH_2)(\mu\text{-}PPh_2)$. In later papers novel chemistry of the μ_3-allenyl and μ-methylene clusters is developed. A preliminary communication on part of this work has appeared.[14]

Experimental Section

All operations and syntheses were performed by using Schlenk techniques under a blanket of nitrogen. Solvents used were stored over an appropriate drying agent and distilled under nitrogen prior to use. Diazomethane was prepared according to standard procedures[15] using N-methyl-N-nitroso-p-toluenesulfonamide (Aldrich Chemical Co.). $Ru_3(CO)_{12}$ was obtained from Strem Chemicals and dried in vacuo prior to use. $PPh_2C{\equiv}C(i\text{-}Pr)$ was synthesized as previously described.[16]

Infrared spectra were measured on Perkin-Elmer 180 and 983 spectrometers using matched NaCl solution cells of 0.5-mm path length. NMR spectra were recorded on Bruker AM-250 (^1H, 250 MHz; ^{31}P, 101.3 MHz; ^{13}C, 62.8 MHz) and WH-400 (^1H, 400 MHz; ^{31}P, 162.0 MHz; ^{13}C, 100.4 MHz) spectrometers. Chemical shifts were referenced to TMS for ^1H and ^{13}C and are relative to 85% H_3PO_4 (external) for ^{31}P. Microanalyses were carried out by the Guelph Chemical Laboratory.

Preparation of $Ru_3(CO)_{11}\{(PPh_2C{\equiv}C(i\text{-}Pr)\}$ (1a). To a flame-dried, 500-mL round-bottom flask equipped with a magnetic stirring bar was added $Ru_3(CO)_{12}$ (2.00 g, 3.13 mmol), THF (270 mL), and $PPh_2C{\equiv}C(i\text{-}Pr)$ (0.79 g, 3.13 mmol). With rapid stirring a catalytic amount of purple, sodium benzophenone ketyl solution was added resulting in a color change from orange to red. Stirring was maintained for approximately 5 minutes, and then solvent was removed until a volume of ca. 10 mL remained. The resulting sludge was diluted with 20–30 mL of heptane and the mixture again concentrated to a final volume of ca. 10 mL. This sludge was then chromatographed on a Florisil column. Eluting with heptane gave a yellow, first band of $Ru_3(CO)_{12}$, a red, second band of **1a**, and a less mobile red, third band of $Ru_3(CO)_{10}\{PPh_2C{\equiv}C(i\text{-}Pr)\}_2$. Yields of $Ru_3(CO)_{12}$ and $Ru_3(CO)_{10}\{PPh_2C{\equiv}C(i\text{-}Pr)\}_2$ were generally well below 10% while yields of $Ru_3(CO)_{11}\{PPh_2C{\equiv}C(i\text{-}Pr)\}$ were from 80 to 90% (as an oil). **1a**: IR ν(CO) (C_6H_{12}) 2096 w, 2044 vs, 2028 s, 2013 vs, 1994 w, 1985 w, 1975 w, sh, 1962 vw, sh cm^{-1}. NMR: $^{31}P\{^1H\}$ (benzene-d_6) 3.1; $^{13}C\{^1H\}$ (benzene-d_6) δ 21.8 (s, CH_3), 22.2 (s, $CH(CH_3)_2$), 74.0 (d, J_{PC} = 96.6 Hz, $C{\equiv}C(i\text{-}Pr)$), 120.2 (d, J_{PC} = 15.2 Hz, $C{\equiv}C(i\text{-}Pr)$), 129.0 (d, J_{PC} = 9.1 Hz, C_m), 130.7 (s, C_p), 131.0 (d, J_{PC} = 12.2 Hz, C_o), 135.8 (d, J_{PC} = 54.9 Hz, C_i), 204.5 (s, CO). Anal. Calcd for $C_{28}H_{17}O_{11}PRu_3$: C, 38.97; H, 1.28; P, 3.59. Found: C, 39.43; H, 2.21; P, 3.56.

Preparation of $Ru_3(CO)_{11}\{(PPh_2C{\equiv}C(t\text{-}Bu)\}$ (1b). This complex was prepared in a manner entirely analogous to the isopropyl derivative just described. Comparable yields were obtained. **1b**: IR ν(CO) (C_6H_{12}) 2096 w, 2044 vs, 2028 s, 2014 s, 1993 w, 1984 w, 1975 w, sh, 1960 w, sh cm^{-1}. NMR: $^{31}P\{^1H\}$ (benzene-d_6) 2.5 (s); $^{13}C\{^1H\}$ (chloroform-d) 204.0 (s, CO), 135.8 (d, $^1J_{PC}$ = 53.5 Hz, C_i), 130.6 (d, $^2J_{PC}$ = 13.6 Hz, C_o), 128.7 (d, $^3J_{PC}$ = 11.7 Hz, C_m), 130.3 (s, C_p), 122.2 (d, $^2J_{PC}$ = 12.9 Hz, C_β), 72.5 (d, $^1J_{PC}$ = 96.1 Hz, C_α), 30.0 (s, CH_3), 29.1 (s, CMe_3). Anal. Calcd for $C_{29}H_{19}O_{11}PRu_3$: C, 39.68; H, 2.18. Found: C, 39.59; H, 2.15.

Preparation of $Ru_3(CO)_9\{\mu_3\text{-}\eta^2\text{-}C{\equiv}C(i\text{-}Pr)\}(\mu\text{-}PPh_2)$ (2a). To the oily mass of $Ru_3(CO)_{11}\{PPh_2C{\equiv}C(i\text{-}Pr)\}$ (**1a**) obtained via the above procedure was added 10 mL of THF, and the solution was transferred to a 250-mL Schlenk type Erlenmeyer Flask. This solution was then diluted to ca. 200 mL with THF and placed in a water bath held at a temperature of 8–10 °C. Nitrogen was bubbled through the solution for a total period of 10–11 days and the mixture worked up as follows: every 2–3 days the nitrogen flow was stopped and CO bubbled through the solution for 1 min. The THF was stripped off until a moist sludge remained. To this was added 30 mL of pentane which resulted in the rapid precipitation of **2a**. The liquor was decanted from the solids and saved. The solids were washed with pentane until the washings were clear and light yellow in color. These washings were collected and added to the mother liquor while the greenish yellow precipitate of **2a** was scooped out of the flask and allowed to air dry on filter paper. The pentane was evaporated from the combined washings and mother liquor and subsequently diluted with ca. 200 mL of THF. The reaction was allowed to proceed further as previously described.

With use of this method a total yield of 1.64 g of **2a** was obtained (65% based on $Ru_3(CO)_{12}$). IR: ν(CO) (C_6H_{12}) 2083 w, 2060 vs, 2042 s, 2013 s, 2009 m, sh, 1994 m, 1984 m, 1977 w, sh cm^{-1}. NMR: $^{31}P\{^1H\}$ (benzene-d_6) δ −73.6. Anal. Calcd for $C_{26}H_{17}O_9PRu_3$: C, 38.67; H, 2.12; P, 3.83. Found: C, 38.94; H, 2.36; P, 4.42.

Preparation of $Ru_3(CO)_9\{\mu_3\text{-}\eta^2\text{-}C{\equiv}C(t\text{-}Bu)\}(\mu\text{-}PPh_2)$ (2b). Satisfactory yields of this cluster could not be obtained by using the method described for the isopropyl analogue.

A solution of $Ru_3(CO)_{11}\{PPh_2C{\equiv}C(t\text{-}Bu)\}$ (0.80 g, 0.94 mmol) in heptane (100 mL) was cooled to −10 °C, and a solution of Me_3NO (0.14 g, 1.8 mmol) in absolute ethanol (10 mL) was added rapidly. The flask was evacuated and allowed to sit overnight at −10 °C. The mother liquor was decanted from the precipitate and saved. A third equivalent of amine oxide (0.07 g, 0.9 mmol) was added to this solution and again stored under vacuum at −10 °C overnight whereupon the precipitate was isolated. The combined solids were recrystallized from heptane under an atmosphere of carbon monoxide to give a yield of 15–20% of $Ru_3(CO)_9\{\mu_3\text{-}\eta^2\text{-}C{\equiv}C(t\text{-}Bu)\}(PPh_2)$ as greenish yellow crystals. IR (C_6H_{12}): ν(CO) 2083 w, 2060 vs, 2042 s, 2013 s, 2009 m, sh, 1994 m, 1984 m, 1977 w, sh cm^{-1}. NMR: $^{31}P\{^1H\}$ (benzene-d_6) δ −73.3 (s). Anal. Calcd for $C_{27}H_{19}O_9PRu_3$: C, 39.47; H, 2.33. Found: C, 39.23; H, 1.66.

Preparation of $Ru_3(CO)_6(\mu\text{-}CO)_2\{\mu_3\text{-}\eta^2\text{-}C{\equiv}C(t\text{-}Bu)\}(\mu\text{-}PPh_2)$ (3b). $Ru_3(CO)_6(\mu\text{-}CO)_2(\mu_3\text{-}\eta^2\text{-}C{\equiv}C(t\text{-}Bu))(\mu\text{-}PPh_2)$ (**3b**) was

---

(5) (a) Yasufuku, K.; Yamazaki, H. *J. Organomet. Chem.* **1972**, *35*, 367. (b) Smith, W. F.; Taylor, N. J.; Carty, A. J. *J. Chem. Soc., Chem. Commun.* **1976**, 896.

(6) For example, alkylation: Yu, Y. F.; Galluci, J.; Wojcicki, A. *J. Am. Chem. Soc.* **1983**, *105*, 4826.

(7) For example, CH_3^+, H^+, and acetylenes see: (a) Geoffroy, G. L.; Rosenberg, S.; Shulman, P. M.; Whittle, R. R. *J. Am. Chem. Soc.* **1984**, *106*, 1519. (b) Regragui, R.; Dixneuf, P. H.; Taylor, N. J.; Carty, A. J. *Organometallics* **1984**, *106*, 1519. (c) Regragui, R.; Dixneuf, P. H.; Taylor, N. J.; Carty, A. J. *Organometallics* **1984**, *3*, 814.

(8) (a) Carty, A. J.; Mott, G. N.; Taylor, N. J. *J. Organomet. Chem.* **1981**, *212*, C54. (b) Carty, A. J.; Taylor, N. J.; Smith, W. F.; Lappert, M. F.; Pye, P. L. *J. Chem. Soc. Chem. Commun.* **1978**, 1017.

(9) Carty, A. J.; Mott, G. N.; Taylor, N. J.; Yule, J. E. *J. Am. Chem. Soc.* **1978**, *100*, 351.

(10) Carty, A. J.; Mott, G. N.; Taylor, N. J.; Ferguson, G.; Khan, M. A.; Roberts, P. J. *J. Organomet. Chem.* **1978**, *149*, 345.

(11) Cherkas, A. A.; Carty, A. J.; Sappa, E.; Pellinghelli, M. S.; Tiripicchio, A. *Inorg. Chem.* **1987**, in press.

(12) Rosen, R. P.; Hoke, J. B.; Whittle, R. R.; Geoffroy, G. L.; Hutchinson, J. P.; Zubieta, J. A. *Organometallics* **1984**, *3*, 846.

(13) (a) Richter, F.; Vahrenkamp, H. *Organometallics* **1982**, *1*, 756. (b) Carty, A. J.; MacLaughlin, S. A.; Taylor, N. J. *J. Organomet. Chem.* **1981**, *204*, C27. (c) MacLaughlin, S. A.; Taylor, N. J.; Carty, A. J. *Organometallics* **1983**, *2*, 1194.

(14) Nucciarone, D.; Taylor, N. J.; Carty, A. J. *Organometallics* **1984**, *3*, 177.

(15) DeBoer, J. J.; Backer, H. J. *Org. Synth.* **1956**, *36*, 16.

(16) Carty, A. J.; Hota, N. K.; Ng, T. W.; Patel, H. A.; O'Connor, T. J. *Can. J. Chem.* **1971**, *49*, 2706.

Table I. Summary of Crystal Data, Intensity Collection, Reduction, and Refinement

	2a	**3b**	**4**	**5**
formula	$C_{26}H_{17}O_9PRu_3$	$C_{26}H_{19}O_8PRu_3 0{\cdot}5C_6H_6$	$C_{26}H_{19}O_8PRu_3$	$C_{26}H_{21}O_7PRu_3$
mol wt	807.60	832.68	793.62	779.64
crystl system	monoclinic	triclinic	monoclinic	monoclinic
space group	$P2_1/c$	$P\bar{1}$	$P2_1/c$	$P2_1/c$
a, Å	13.189 (1)	9.674 (1)	11.892 (2)	11.890 (2)
b, Å	9.674 (1)	13.373 (1)	12.200 (2)	11.973 (1)
c, Å	22.481 (2)	13.654 (1)	19.698 (4)	19.675 (2)
α, deg	90	108.97 (1)	90	90
β, deg	91.82 (1)	72.64 (1)	93.22 (2)	90.10 (2)
γ, deg	90	93.79 (1)	90	90
Z	4	2	4	4
V, Å^3	2866.9 (5)	1593.6 (3)	2853 (1)	2900.9 (6)
d(calcd), g·cm^{-3}	1.871	1.735	1.847	1.849
d(measd), g·cm^{-3}	1.82	1.74	1.85	1.85
μ(Mo Kα), cm^{-1}	16.29	14.70	16.32	16.58
radiatn	graphite-monochromated Mo Kα (λ = 0.71069 Å)			
diffractometer	Syntex $P2_1$			
cryst size, mm	0.23 × 0.23 × 0.27	0.20 × 0.25 × 0.26	0.19 × 0.22 × 0.23	0.17 × 0.17 × 0.27
scan type	$\theta/2\theta$	$\theta/2\theta$	$\theta/2\theta$	$\theta/2\theta$
2θ range, deg	≤ 45	≤ 45	≤ 46	≤ 50
scan speed	variable 2.93–29.3° min^{-1}			
scan width	0.8° below Kα_1 to 0.8° above Kα_2			
std reflctns	$51\bar{3}$, 208	$3\bar{7}\bar{1}$, 254	308, $50\bar{6}$	304, $32\bar{2}$
change in stds (%)	±2	±2	±1	±6
data measd	3785	5632	3997	4957
data obsd ($I \geq 3\sigma(I)$)	2743	4911	3007	3339
transmissn factors	0.60–0.76	0.64–0.79	0.63–0.79	0.65–0.79
no. of variables	421	447	420	419
$R = \sum(\lvert F_o\rvert - \lvert F_c\rvert)/\sum\lvert F_o\rvert$	0.025	0.028	0.029	0.035
$R_w = [\sum w(\lvert F_o\rvert - \lvert F_c\rvert)^2/\sum w\lvert F_o\rvert^2]^{1/2}$	0.028	0.034	0.031	0.039
weighting scheme	$w^{-1} = 0.85 - 0.0044\lvert F_o\rvert + 0.00004\lvert F_o\rvert^2$	$w^{-1} = 2.2 - 0.0275\lvert F_o\rvert + 0.00078\lvert F_o\rvert^2$	$w^{-1} = 1.9 - 0.0185\lvert F_o\rvert + 0.00015\lvert F_o\rvert^2$	$w^{-1} = 1.89 - 0.0173\lvert F_o\rvert + 0.00017\lvert F_o\rvert^2$
electron density level final difference map (e Å^{-3})	0.5	0.65	0.5	0.6

prepared by bubbling nitrogen gas through a heptane solution of **2b** at room temperature until the infrared spectra indicated complete disappearance of starting material. **3b**: IR (C_6H_{12}): ν(CO) 2060 m, 2028 s, 2018 s, 1996 m, 1981 m, 1969 m, 1948 w, 1847 w cm^{-1}. NMR: $^{31}P\{^1H\}$ (benzene-d_6) δ 334.9. Anal. Calcd for $C_{26}H_{19}O_8PRu_3$: C, 39.35; H, 2.41. Found: C, 38.95; H, 2.59.

Preparation of $Ru_3(CO)_8\{\mu_3\text{-}\eta^3\text{-}CH_2C_2(i\text{-}Pr)\}(\mu\text{-}PPh_2)$ (4). To a 250-mL, three-necked, round-bottom flask equipped with a magnetic stirring bar was added $Ru_3(CO)_9\{\mu_3\text{-}\eta^2\text{-}C{\equiv}C(i\text{-}Pr)\}(\mu\text{-}PPh_2)$ (200 mg, 0.248 mmol) and heptane (100 mL). With nitrogen bubbling through the solution the flask was immersed in an oil bath heated at 60 °C and left stirring for 6 h with solvent being replenished as required. Heating was stopped, the flask cooled in an ice-bath, and the nitrogen purge removed. To this rapidly stirring solution was added 3–5 mL of ca. 0.4 M diazomethane/ether solution. The bath was removed and the solution allowed to reach room temperature. The solution was concentrated to a volume of 10 mL and chromatographed on Florisil. Eluting with heptane gave a yellow, first band containing small amounts of $Ru_3(CO)_{12}$ and $Ru_2(CO)_6\{\mu\text{-}\eta^2\text{-}C_2(i\text{-}Pr)\}(\mu\text{-}PPh_2)$ (impurities in starring material), followed by a gray, second band of $Ru_3(CO)_7(\mu\text{-}CH_2)\{\mu_3\text{-}\eta^3\text{-}CH_2C_2(i\text{-}Pr)\}(\mu\text{-}PPh_2)$ and a maroon, third band of $Ru_3(CO)_8\{\mu_3\text{-}\eta^3\text{-}CH_2C_2(i\text{-}Pr)\}(\mu\text{-}PPh_2)$. Concentration of the third band followed by refrigeration at −15 °C gave crystalline $Ru_3(CO)_8\{\mu_3\text{-}\eta^3\text{-}CH_2C_2(i\text{-}Pr)\}(\mu\text{-}PPh_2)$ (4) in 30–35% yields. IR (C_6H_{12}): ν(CO) 2075 m, 2047 s, 2018 m, 2007 m, 1996 w, 1989 w, 1975 w, 1946 m cm^{-1}. NMR: $^{31}P\{^1H\}$ ($CDCl_3$, −40 °C) δ 269.4 (s); ^{13}C ($CDCl_3$, −60 °C) δ 210.9 (s, CO), 200.7 (s, CO), 197–195 (m, 4CO), 194.8 (s, CO), 193.4 (d, CO, $^2J_{PC}$ = 73 Hz), 172.0 (s, C(11)), 142.7 (s, C(10)), 140.6 (d, ipso-CPh, $^1J_{PC}$ = 30 Hz), 134.6 (d, ipso-CPh, $^1J_{PC}$ = 30 Hz), 133–128 (m, phenyls), 43.8 (d, C(12), $^1J_{CH}$ = 131 Hz), 24.8 (q, Me, $^1J_{CH}$ = 126 Hz), 23.6 (q, Me, $^1J_{CH}$ = 126 Hz), 20.1 (t, C(9), $^1J_{CH}$ = 161 Hz); ^1H ($CDCl_3$, −60 °C) δ 1.22 (d, 3 H, J = 7 Hz), 1.25 (d, 3 H, J = 7 Hz), 1.65 (d, 1 H, J = 4 Hz), 1.67 (d, 1 H, J = 4 Hz), 3.04 (m, 1 H, J = 7 Hz), 7.3–7.6 (10 H). Anal. Calcd for $C_{26}H_{19}O_8PRu_3$: C, 39.35; H, 2.41. Found: C, 39.45; H, 2.59.

Preparation of $Ru_3(CO)_7(\mu\text{-}CH_2)\{\mu_3\text{-}\eta^3\text{-}CH_2C_2(i\text{-}Pr)\}(\mu\text{-}PPh_2)$ (5). To a 250-mL two-necked round-bottom flask equipped with a magnetic stirring bar was added $Ru_3(CO)_8\{\mu_3\text{-}\eta^3\text{-}CH_2C_2(i\text{-}Pr)\}(\mu\text{-}PPh_2)$ (4) (65 mg, 0.082 mmol) and heptane (50 mL). The solution was cooled to −30 °C, and ethereal diazomethane was added in ca. 1-mL portions until monitoring by IR of reaction aliquots indicated complete consumption of starting material. The solution was concentrated to a volume of ca. 5 mL, transferred to a Schlenk tube, and set aside for crystallization by refrigeration at −15 °C. Crystallization was aided by addition of a seed crystal. In this manner 52 mg of black crystals of $Ru_3(CO)_7(\mu\text{-}CH_2)\{\mu_3\text{-}\eta^3\text{-}CH_2C_2(i\text{-}Pr)\}(\mu\text{-}PPh_2)$ (5) was obtained (81%). IR (C_6H_{12}): ν(CO) 2064 m, 2025 m, 2011 s, 1973 w, 1953 m cm^{-1}. NMR: $^{31}P\{^1H\}$ (CD_3COCD_3, −65 °C) δ 139.3; ^1H ($CDCl_3$, −60 °C) δ 0.99 (d, J = 5.9 Hz, CH_3), 1.02 (d, J = 6.6 Hz, CH_3), 2.46 (m, J = 6.3 Hz, $CH(CH_3)_2$, 2.76 (s, 1 H, μ-CH_2), 2.79 (s, 1 H, μ-CH_2), 6.19 (s, 2 H, CH_2), 7.29–7.41 (m, 10 H). Anal. Calcd for $C_{26}H_{21}O_7PRu_3$: C, 40.05; H, 2.72. Found: C, 39.81; H, 2.56.

X-ray Crystal Structure Analyses. The structures of $Ru_3(CO)_9\{\mu_3\text{-}\eta^2\text{-}C{\equiv}C(i\text{-}Pr)\}(\mu\text{-}PPh_2)$ (**2a**), $Ru_3(CO)_6(\mu\text{-}CO)_2\{\mu_3\text{-}\eta^2\text{-}C{\equiv}C(t\text{-}Bu)\}(\mu\text{-}PPh_2)$ (**3b**), $Ru_3(CO)_8\{\mu_3\text{-}\eta^3\text{-}CH_2CC(i\text{-}Pr)\}(\mu\text{-}PPh_2)$ (4), and $Ru_3(CO)_7(\mu\text{-}CH_2)\{\mu_3\text{-}\eta^3\text{-}CH_2CC(i\text{-}Pr)\}(\mu\text{-}PPh_2)$ (**5**) were determined. Unit cell data, intensity collection, reduction, and refinement are given in Table I. Colors, crystal form, and crystallization solvents were as follows: **2a**, yellow-green prisms from heptane; **3b**, orange-red needles from heptane to which a few drops of benzene had been added; **4**, maroon prisms from heptane; **5**, gray needles from heptane. Diffraction measurements were carried out at 23 ± 2 °C on a Syntex $P2_1$ diffractometer. In each case a suitable crystal was attached to a glass fiber with epoxy glue, and mounted on a brass pin in a goniometer head and its diffraction characteristics were examined via a random orientation, polaroid rotation photograph. Data from the rotation photograph were input into the Data General Nova control computer to generate possible unit cells. Axial photographs taken about the axes of the chosen cell were used as a further check of cell solutions. Accurate unit cell dimensions were obtained from least-squares fitting of 2θ, ω, and χ values of 15 well-centered, reasonably intense reflections selected from diverse regions of reciprocal space.

Intensity data were collected by using a coupled θ(crystal)–

2θ(counter) scan with a scan rate set to optimize measurements for weak and strong reflections. Background counts were measured at the beginning and end of the scan for half of the scan time. Standards were monitored after every 100 measurements. Only data for 5 needed correction for decay. Lorentz and polarization corrections were applied to all data. Due to the low values of μ and the almost equidimensional nature of the crystals no absorption corrections were applied.

In each case the structures were solved by a combination of Patterson, Fourier, and least-squares methods. Scattering factors employed were taken from ref 17 with the exception of data for hydrogen atoms where the compilations of Stewart et al.[18] were used. Both real ($\Delta F'$) and imaginary ($\Delta F''$) components of anomalous dispersion for heavy atoms were included. Intensity data for all four compounds were of sufficient quality to permit the location of hydrogen atoms via difference Fourier syntheses. Usually difference Fourier maps were calculated subsequent to several cycles of least-squares refinement with all heavy atoms having anisotropic thermal parameters. In the last stages hydrogen atoms were included and positions and an isotropic temperature factor varied.

The function minimized in least-squares refinements was $\sum_w \Delta |F|^2$. Computations were carried out on IBM 4341 systems in the University of Waterloo Computing Center. Programs used have been described elsewhere.[9] Atomic coordinates for **2a**, **3b**, **4**, and **5** are listed in Table II, IV, VI, and VIII, respectively, with a selection of important bond lengths and angles included as Table III, V, VII, and IX.

Complete listings of anisotropic thermal parameters (Tables S1–S4), remaining bond lengths and angles (Tables S5–S8), and structure factors (Tables S9–S12) have been deposited as supplementary data.

Results and Discussion

Synthetic Aspects. A brief report on the synthesis and characterization of $Ru_3(CO)_9\{\mu_3\text{-}\eta^2\text{-}C{\equiv}C(i\text{-}Pr)\}(\mu\text{-}PPh_2)$ (**2a**) was published in an earlier communication.[13b] We have since found that the synthetic route described herein provides better yields and more consistent results. The only drawback appears to be the length of time required to accumulate workable quantities of **2a**. However replenishment of partially spent solutions with **1a** provides a continuing source of **2a** until such time as the buildup of side products leads to coprecipitation with **2a**. Although the reaction can be carried out at room temperature, yields are reduced to 30–40%. Lower temperatures result in significantly less decomposition of **2a**, but its rate of formation from **1a** is also reduced. Rapid purging of the solutions with nitrogen also leads to improved yields presumably due to removal of CO from the reaction atmosphere. The overall synthetic route to **2a** from $Ru_3(CO)_{12}$ is given by eq 1.

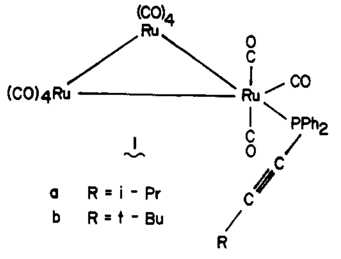

1

a R = i - Pr

b R = t - Bu

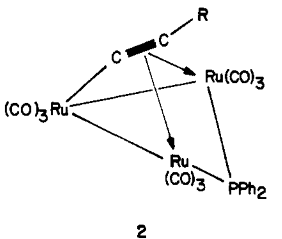

2

a R = i - Pr

b R = t - Bu

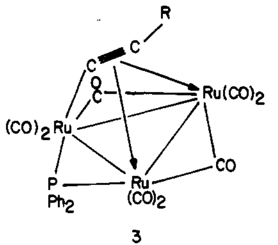

3

a R = i - Pr

b R = t - Bu

$$Ru_3(CO)_{12} + PhPC{\equiv}C(i\text{-}Pr) \xrightarrow{-CO} Ru_3(CO)_{11}\{Ph_2PC{\equiv}C(i\text{-}Pr)\} \xrightarrow{-2CO} Ru_3(CO)_9\{\mu_3\text{-}\eta^2\text{-}C{\equiv}C(i\text{-}Pr)\}(\mu\text{-}PPh_2) \quad (1)$$

Minor products produced in this reaction include $Ru_2(CO)_6\{(\mu\text{-}\eta^2\text{-}C{\equiv}C(i\text{-}Pr)\}(\mu\text{-}PPh_2)$ and $Ru_5(CO)_{13}\{\mu_4\text{-}\eta^2\text{-}C{\equiv}C(i\text{-}Pr)\}(\mu\text{-}PPh_2)$, both of which have been described elsewhere.[1b,13b] In the case of the *tert*-butyl acetylide the synthesis of **2b** requires the use of Me_3NO to displace CO in the final step.

The synthesis of $Ru_3(CO)_8\{\mu_3\text{-}\eta^3\text{-}CH_2CC(i\text{-}Pr)\}(\mu\text{-}PPh_2)$ (**4**) from **2a** and diazomethane requires initial conversion of 50-electron **2a** to 48-electron $Ru_3(CO)_6(\mu\text{-}CO)_2\{(\mu_3\text{-}\eta^2\text{-}C{\equiv}C(i\text{-}Pr)\}(\mu\text{-}PPh_2)$ (**3a**) (eq 2) followed by coordination of CH_2N_2 (or CH_2) at a reactive site on the cluster.

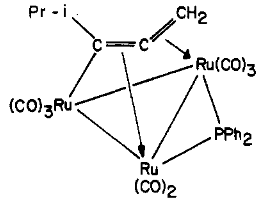

4

$$\underset{\mathbf{2a}}{Ru_3(CO)_9\{\mu_3\text{-}\eta^2\text{-}C{\equiv}C(i\text{-}Pr)\}(\mu\text{-}PPh_2)} \xrightarrow{-CO} \underset{\mathbf{3a}}{Ru_3(CO)_6(\mu\text{-}CO)_2\{\mu_3\text{-}\eta^2\text{-}C{\equiv}C(i\text{-}Pr)\}(\mu\text{-}PPh_2)} + CO \quad (2)$$

Justification for this reaction pathway can be summarized as follows: (i) Complex **2a** can be converted in 90% yield to **3a** by bubbling a stream of dinitrogen through a heated (60 °C) solution of **2a** in *n*-heptane. Infrared monitoring shows the disappearance of peaks due to **2a** and their replacement by bands of the carbonyl-bridged cluster **3a**. Freshly prepared solutions of **3a** react within seconds, even at −40 °C, with ethereal diazomethane. In contrast, pure **2a** reacts only very sluggishly with **2a** affording **3a**. Reaction of **2a** with CH_2N_2 is inhibited by saturation of solutions with CO gas. (ii) The osmium analogue of **2a**, $Os_3(CO)_9\{\mu_3\text{-}\eta^2\text{-}C{\equiv}C(i\text{-}Pr)\}(\mu\text{-}PPh_2)$ which does not convert to $Os_3(CO)_6(\mu\text{-}CO)_2\{\mu_3\text{-}\eta^2\text{-}C{\equiv}C(i\text{-}Pr)\}(\mu\text{-}PPh_2)$ in solution[13b] does not react at all with CH_2N_2 at room temperature. (iii) The μ-hydrido, μ-acetylide cluster $(\mu\text{-}H)Ru_3(CO)_9\{\mu_3\text{-}\eta^2\text{-}C{\equiv}C(t\text{-}Bu)\}$,[19] which is related to **2a** by replacing a μ-PPh_2 group by a hydride and an Ru–Ru bond, is also quite unreactive toward CH_2N_2. Unlike **3a**, this hydride does not react with CO to give an open-edged 50-electron species, and in addition it is relatively stable to substitution.

---

(17) *International Tables for X-ray Crystallography*; Kynoch: Birmingham, England, 1974; Vol. IV.

(18) Stewart, R. F.; Davidson, E. R.; Simpson, W. T. *J. Chem. Phys.* **1965**, *42*, 3175.

(19) (a) Sappa, E.; Gambino, O.; Milone, L.; Cetini, G. *J. Organomet. Chem.* **1972**, *39*, 169. (b) Catti, M.; Gervasio, G.; Mason, S. A. *J. Chem. Soc.*, Dalton *Trans.* **1977**, 2660.

These observations also lead us to suggest that transfer of the methylene unit to the α-carbon atom of the acetylide in **3a** proceeds via prior activation on the metal framework of coordinated CH_2N_2 or methylene (CH_2) intermediates rather than via direct attack by CH_2N_2 on the α-carbon atom. Additional indirect support for this is the fact that direct attack at acetylidic carbon of the stable clusters $Os_3(CO)_9(\mu_3\text{-}\eta^2\text{-}C{\equiv}CPh)(\mu\text{-}PPh_2)$ and $(\mu\text{-}H)Ru_3(CO)_9(\mu_3\text{-}\eta^2\text{-}C{\equiv}CPh)$ *does* occur wtih *t*-BuNC.[20]

The overall yields of the allenyl cluster $Ru_3(CO)_8\{\mu_3\text{-}\eta^2\text{-}CH_2C_2(i\text{-}Pr)\}(\mu\text{-}PPh_2)$ (**4**) from **3a** (or **2a**) and CH_2N_2 (eq 3) are modest. Contributing to this is the fact that the

$$\underset{\mathbf{3a}}{Ru_3(CO)_6(\mu\text{-}CO)_2\{\mu_3\text{-}\eta^2\text{-}C{\equiv}C(i\text{-}Pr)\}(\mu\text{-}PPh_2)} + CH_2N_2 \xrightarrow{-N_2} \underset{\mathbf{4}}{Ru_3(CO)_8\{\mu_3\text{-}\eta^3\text{-}CH_2C_2(i\text{-}Pr)\}(\mu\text{-}PPh_2)} \tag{3}$$

reaction does not stop at the formation of **4** but proceeds further to afford the μ-methylene complex **5** (eq 4). In-

$$Ru_3(CO)_8\{\mu_3\text{-}\eta^3\text{-}CH_2C_2(i\text{-}Pr)\}(\mu\text{-}PPh_2) + CH_2N_2 \xrightarrow{-N_2} \underset{\mathbf{5}}{Ru_3(CO)_7\{\mu_3\text{-}\eta^3\text{-}CH_2C_2(i\text{-}Pr)\}(\mu\text{-}CH_2)(\mu\text{-}PPh_2)} \tag{4}$$

deed independent isolation of **4** and subsequent reaction with CH_2N_2 leads to rapid and quantitative (IR) formation of **5** even at −30 °C. Complex **4** is stable in the solid state and undergoes only slow decomposition in hydrocarbon solvents. The μ-methylene complex **5** is much more fragile and undergoes a number of interesting reactions including an intramolecular isomerization to the butadienediyl cluster $(\mu\text{-}H)Ru_3(CO)_7\{\mu_3\text{-}\eta^4\text{-}CH_2CC(i\text{-}Pr)CH\}(\mu\text{-}PPh_2)$ on standing in solution under N_2. It must therefore be isolated quickly to avoid decomposition. The chemistry of **5** is the focus of a following paper.

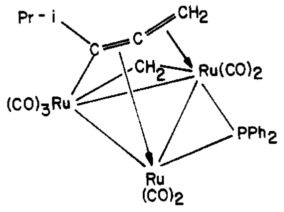

5

In summary the seemingly poor yields of **4** can now be explained by sorting out the reactions which occur upon addition of CH_2N_2 to heptane solutions of **3a**. The first reaction which occurs is described by eq 3. Since the product from eq 3 also reacts with CH_2N_2 via eq 4, yields of **4** must, as a consequence, be reduced. Further reduction in yield is noted as a result of the release of CO in eq 3. This CO can react with **3a**, as described in eq 2, and thus reduce the amount of **3a** available for reaction with CH_2N_2. These two factors, coupled with decomposition noted in the formation of **3a**, are probably the major reasons why modest yields of **4** are obtained.

Table II. Atomic Coordinates (Fractional ×10^4) and Hydrogen Atom Thermal Parameters for $Ru_3(CO)_9\{\mu_3\text{-}\eta^2\text{-}C{\equiv}C(i\text{-}Pr)\}(\mu\text{-}PPh_2)$ (2a)

(a) Heavy Atoms

atom	*x*	*y*	*z*
Ru(1)	2712.1 (4)	−196.8 (5)	1102.0 (2)
Ru(2)	954.1 (4)	780.4 (5)	1650.6 (2)
Ru(3)	1968.0 (4)	3213.8 (5)	1268.0 (2)
P	3404.7 (10)	1848.7 (15)	1562.8 (6)
O(1)	2996 (4)	−2297 (5)	2097 (2)
O(2)	4729 (3)	−705 (5)	505 (2)
O(3)	1497 (4)	−2415 (5)	404 (2)
O(4)	1540 (4)	630 (6)	2982 (2)
O(5)	−1037 (4)	2274 (7)	1832 (3)
O(6)	91 (4)	−2123 (6)	1633 (3)
O(7)	1501 (4)	4351 (6)	2484 (2)
O(8)	3267 (4)	5661 (5)	890 (2)
O(9)	−36 (4)	4465 (7)	764 (3)
C(1)	2897 (5)	−1470 (6)	1739 (3)
C(2)	3963 (5)	−520 (6)	708 (2)
C(3)	1952 (5)	−1609 (6)	666 (3)
C(4)	1313 (5)	688 (7)	2496 (3)
C(5)	−285 (5)	1717 (8)	1770 (3)
C(6)	405 (5)	−1024 (8)	1639 (3)
C(7)	1697 (5)	3880 (7)	2041 (3)
C(8)	2785 (5)	4722 (6)	1014 (3)
C(9)	693 (5)	4006 (7)	946 (3)
C(10)	1404 (4)	1222 (6)	850 (3)
C(11)	2062 (4)	1597 (6)	473 (2)
C(12)	2260 (6)	1819 (8)	−180 (3)
C(13)	1716 (8)	3104 (10)	−415 (4)
C(14)	1950 (8)	559 (9)	−541 (4)
C(15)	3755 (4)	1906 (6)	2359 (2)
C(16)	4032 (5)	734 (7)	2675 (3)
C(17)	4310 (5)	825 (7)	3277 (3)
C(18)	4322 (5)	2079 (7)	3560 (3)
C(19)	4091 (5)	3252 (7)	3244 (3)
C(20)	3811 (5)	3166 (6)	2648 (3)
C(21)	4628 (4)	2339 (5)	1255 (2)
C(22)	5533 (4)	2113 (6)	1566 (3)
C(23)	6457 (5)	2424 (8)	1317 (4)
C(24)	6490 (6)	2998 (8)	754 (4)
C(25)	5595 (5)	3228 (7)	436 (3)
C(26)	4677 (5)	2891 (6)	677 (3)

(b) Hydrogen Atoms

	x	*y*	*z*	U_{iso}, Å^2
H(12)	302 (5)	199 (7)	−25 (3)	59 (16)
H(13A)	192 (5)	315 (7)	−86 (3)	131 (32)
H(13B)	109 (6)	316 (9)	−37 (4)	109 (32)
H(13C)	194 (6)	392 (8)	−23 (3)	84 (23)
H(14A)	246 (6)	−15 (8)	−47 (3)	127 (33)
H(14B)	209 (5)	66 (8)	−97 (3)	73 (19)
H(14C)	131 (6)	11 (8)	−52 (3)	95 (27)
H(16)	400 (5)	−17 (7)	250 (3)	43 (14)
H(17)	452 (5)	4 (7)	349 (3)	78 (21)
H(18)	460 (5)	207 (6)	399 (3)	52 (15)
H(19)	397 (5)	423 (7)	342 (3)	56 (16)
H(20)	369 (4)	396 (6)	240 (3)	53 (16)
H(22)	551 (5)	175 (6)	192 (3)	29 (13)
H(23)	701 (5)	222 (7)	151 (3)	80 (22)
H(24)	709 (5)	320 (7)	65 (3)	61 (18)
H(25)	566 (5)	351 (7)	5 (3)	75 (20)
H(26)	407 (4)	307 (6)	42 (3)	50 (16)

While cluster-bound methylene intermediates were not isolated from the reaction depicted in eq 3, the reaction of **4** with CH_2N_2 leads to the isolable μ-methylene cluster. Formation of this cluster might involve initial attack at Ru(3) of **4**. Evidence for this arises from experiments showing that CO readily attacks **4** to give the new, open-edge cluster $Ru_3(CO)_9\{\mu_3\text{-}\eta^3\text{-}CH_2{=}C{=}C(i\text{-}Pr)\}(\mu\text{-}PPh_2)$ (**6**).[21] Labeling studies with ^{13}CO show that the incorporated CO occupies a site trans to the phosphido bridge thus making Ru(3) the only likely site of attack. This

---

[20] MacLaughlin, S. A.; Johnson, J. P.; Taylor, N. J.; Carty, A. J.; Sappa, E. *Organometallics* **1983**, *2*, 352.

[21] Nucciarone, D.; Taylor, N. J.; Carty, A. J. *Organometallics*, third of three papers in this issue.

Table III. A Selection of Important Bond Lengths (Å) and Angles (deg) for $Ru_3(CO)_9\{\mu_3\text{-}\eta^2\text{-}C{\equiv}C(i\text{-}Pr)\}(\mu\text{-}PPh_2)$ (2a)

(a) Bond Lengths

Ru(1)–Ru(2)	2.8235 (7)	Ru(1)···Ru(3)	3.4658 (6)
Ru(1)–P	2.401 (1)	Ru(1)–C(1)	1.898 (6)
Ru(1)–C(2)	1.922 (6)	Ru(1)–C(3)	1.941 (6)
Ru(1)–C(10)	2.262 (5)	Ru(1)–C(11)	2.381 (5)
Ru(2)–Ru(3)	2.8535 (6)	Ru(2)–C(4)	1.946 (7)
Ru(2)–C(5)	1.895 (7)	Ru(2)–C(6)	1.890 (7)
Ru(2)–C(10)	1.960 (6)	Ru(3)–P	2.386 (1)
Ru(3)–C(7)	1.899 (7)	Ru(3)–C(8)	1.913 (6)
Ru(3)–C(9)	1.965 (7)	Ru(3)–C(10)	2.259 (6)
Ru(3)–C(11)	2.381 (5)	P–C(15)	1.836 (5)
P–C(21)	1.839 (5)	C(1)–O(1)	1.139 (8)
C(2)–O(2)	1.137 (7)	C(3)–O(3)	1.138 (8)
C(4)–O(4)	1.125 (9)	C(5)–O(5)	1.141 (9)
C(6)–O(6)	1.141 (9)	C(7)–O(7)	1.132 (9)
C(8)–O(8)	1.148 (8)	C(9)–O(9)	1.125 (9)
C(10)–C(11)	1.284 (8)	C(11)–C(12)	1.515 (8)
C(12)–C(13)	1.520 (9)	C(12)–C(14)	1.513 (11)

(b) Bond Angles

Ru(2)–Ru(1)–P	80.92 (3)	Ru(2)–Ru(1)–C(1)	88.6 (1)
Ru(2)–Ru(1)–C(2)	169.8 (1)	Ru(2)–Ru(1)–C(3)	92.2 (1)
Ru(2)–Ru(1)–C(10)	43.6 (1)	Ru(2)–Ru(1)–C(11)	74.3 (1)
P–Ru(1)–C(1)	99.9 (1)	P–Ru(1)–C(2)	90.7 (1)
P–Ru(1)–C(3)	168.8 (1)	P–Ru(1)–C(10)	83.4 (1)
P–Ru(1)–C(11)	77.3 (1)	C(1)–Ru(1)–C(2)	98.6 (2)
C(1)–Ru(1)–C(3)	88.6 (2)	C(1)–Ru(1)–C(10)	131.4 (2)
C(1)–Ru(1)–C(11)	162.9 (2)	C(2)–Ru(1)–C(3)	95.2 (2)
C(2)–Ru(1)–C(10)	130.0 (2)	C(2)–Ru(1)–C(11)	98.2 (2)
C(3)–Ru(1)–C(10)	85.6 (2)	C(3)–Ru(1)–C(11)	92.4 (2)
C(10)–Ru(1)–C(11)	32.0 (1)	Ru(1)–Ru(2)–Ru(3)	75.25 (1)
Ru(1)–Ru(2)–C(4)	103.5 (1)	Ru(1)–Ru(2)–C(5)	161.0 (2)
Ru(1)–Ru(2)–C(6)	90.3 (2)	Ru(1)–Ru(2)–C(10)	52.8 (1)
Ru(3)–Ru(2)–C(4)	103.3 (1)	Ru(3)–Ru(2)–C(5)	93.6 (2)
Ru(3)–Ru(2)–C(6)	160.2 (2)	Ru(3)–Ru(2)–C(10)	52.1 (1)
C(4)–Ru(2)–C(5)	93.9 (2)	C(4)–Ru(2)–C(6)	93.0 (2)
C(4–)Ru(2)–C(10)	146.7 (2)	C(5)–Ru(2)–C(6)	96.4 (3)
C(5)–Ru(2)–C(10)	108.3 (2)	C(6)–Ru(2)–C(10)	108.4 (2)
Ru(2)–Ru(3)–P	80.53 (3)	Ru(2)–Ru(3)–C(7)	84.3 (2)
Ru(2)–Ru(3)–C(8)	173.5 (1)	Ru(2)–Ru(3)–C(9)	91.7 (2)
Ru(2)–Ru(3)–C(10)	43.2 (1)	Ru(2)–Ru(3)–C(11)	73.8 (1)
P–Ru(3)–C(7)	96.0 (2)	P–Ru(3)–C(8)	93.2 (1)
P–Ru(3)–C(9)	168.7 (2)	P–Ru(3)–C(10)	83.8 (1)
P–Ru(3)–C(11)	77.6 (1)	C(7)–Ru(3)–C(8)	98.0 (2)
C(7)–Ru(3)–C(9)	91.3 (2)	C(7)–Ru(3)–C(10)	126.9 (2)
C(7)–Ru(3)–C(11)	157.8 (2)	C(8)–Ru(3)–C(9)	94.4 (2)
C(8)–Ru(3)–C(10)	135.1 (2)	C(8)–Ru(3)–C(11)	103.5 (2)
C(9)–Ru(3)–C(10)	85.0 (2)	C(9)–Ru(3)–C(11)	92.5 (2)
C(10)–Ru(3)–C(11)	32.0 (1)		
Ru(1)–P–Ru(3)	92.76 (3)	Ru(1)–P–C(15)	121.8 (1)
Ru(1)–P–C(21)	112.1 (1)	Ru(3)–P–C(15)	115.3 (1)
Ru(3)–P–C(21)	116.8 (1)	C(15)–P–C(21)	99.4 (2)
Ru(1)–C(1–)O(1)	175.8 (2)	Ru(1)–C(2)–O(2)	176.2 (2)
Ru(1)–C(3)–O(3)	178.5 (2)	Ru(2)–C(4)–O(4)	178.7 (2)
Ru(2)–C(5)–O(5)	178.7 (3)	Ru(2)–C(6)–O(6)	178.7 (2)
Ru(3)–C(7)–O(7)	175.2 (2)	Ru(3)–C(8)–O(8)	176.3 (2)
Ru(3)–C(9)–O(9)	179.6 (3)	Ru(1)–C(10)–Ru(2)	83.6 (1)
Ru(1)–C(10)–Ru(3)	100.1 (1)	Ru(1)–C(10)–C(11)	79.1 (2)
Ru(2)–C(10)–Ru(3)	84.8 (1)	Ru(2)–C(10)–C(11)	154.0 (2)
Ru(3)–C(10)–C(11)	79.2 (1)	Ru(1)–C(11)–Ru(3)	93.4 (1)
Ru(1)–C(11)–C(10)	68.9 (2)	Ru(1)–C(11)–C(12)	127.5 (2)
Ru(3)–C(11)–C(10)	68.8 (2)	Ru(3)–C(11)–C(12)	130.5 (2)
C(10)–C(11)–C(12)	145.2 (3)	C(11)–C(12)–C(13)	111.0 (3)
C(11)–C(12)–C(14)	110.7 (4)	C(13)–C(12)–C(14)	110.9 (4)

chemistry in fact parallels that observed for the acetylide system described by eq 3. The analogous reaction with CO is described by eq 5.

$$\underset{4}{Ru_3(CO)_8\{\mu_3\text{-}\eta^3\text{-}CH_2{=}C{=}C(i\text{-}Pr)\}(\mu\text{-}PPh_2)} + CO \rightarrow \underset{6}{Ru_3(CO)_9\{\mu_3\text{-}\eta^3\text{-}CH_2{=}C{=}C(i\text{-}Pr)\}(\mu\text{-}PPh_2)} \quad (5)$$

Table IV. Atomic Coordinates (Fractional ×10⁴) and Hydrogen Atom Thermal Parameters for $Ru_3(CO)_6(\mu\text{-}CO)_2\{\mu_3\text{-}\eta^2\text{-}C{\equiv}C(t\text{-}Bu)\}(\mu\text{-}PPh_2)$ (3b)

(a) Heavy Atoms

atom	*x*	*y*	*z*
Ru(1)	192.0 (3)	2634.7 (2)	2204.9 (2)
Ru(2)	1933.9 (4)	3669.2 (3)	799.3 (3)
Ru(3)	3241.1 (3)	2357.8 (2)	1428.7 (2)
P	1670.2 (10)	1820.7 (7)	2821.8 (8)
O(1)	−971 (5)	532 (4)	1105 (4)
O(2)	−2598 (4)	3166 (4)	4027 (3)
O(3)	−1456 (4)	3801 (5)	1238 (4)
O(4)	1823 (6)	5876 (3)	688 (3)
O(5)	1717 (6)	2759 (4)	−1464 (3)
O(6)	5044 (4)	3012 (3)	−585 (3)
O(7)	3713 (5)	301 (3)	−401 (3)
O(8)	6127 (4)	2129 (3)	1805 (4)
C(1)	−565 (5)	1325 (4)	1505 (4)
C(2)	−1551 (4)	2972 (4)	3358 (3)
C(3)	−514 (5)	3476 (5)	1410 (4)
C(4)	1874 (6)	5044 (4)	712 (4)
C(5)	1770 (6)	3112 (4)	−599 (4)
C(6)	4050 (5)	3052 (3)	149 (3)
C(7)	3512 (5)	1054 (3)	322 (4)
C(8)	5058 (4)	2231 (3)	1664 (4)
C(10)	1658 (4)	3778 (3)	2521 (3)
C(11)	2842 (4)	4214 (3)	2400 (3)
C(12)	3887 (4)	5044 (3)	2745 (3)
C(13)	4319 (5)	4816 (4)	3643 (4)
C(14)	3082 (6)	6121 (4)	3190 (5)
C(15)	5232 (5)	5051 (4)	1809 (4)
C(16)	1804 (4)	2481 (3)	4184 (3)
C(17)	966 (4)	3381 (3)	4882 (3)
C(18)	1127 (5)	3885 (4)	5903 (3)
C(19)	2125 (6)	3507 (4)	6236 (4)
C(20)	2979 (7)	2642 (5)	5558 (5)
C(21)	2825 (5)	2115 (4)	4527 (4)
C(22)	1402 (4)	449 (3)	2782 (3)
C(23)	2211 (8)	−362 (4)	1993 (7)
C(24)	1890 (9)	−1412 (5)	1957 (8)
C(25)	838 (7)	−1631 (4)	2713 (6)
C(26)	23 (9)	−829 (5)	3512 (6)
C(27)	316 (8)	214 (4)	3554 (5)
C(S1)	4991 (28)	629 (15)	6436 (18)
C(S2)	6009 (14)	596 (11)	5166 (23)
C(S3)	5976 (22)	118 (16)	4059 (24)

(b) Hydrogen Atoms

atom	*x*	*y*	*z*	U_{iso}, Å^2
H(13A)	340	476	421	78 (15)
H(13B)	487	415	337	83 (15)
H(13C)	484	538	392	80 (14)
H(14A)	279	627	264	89 (16)
H(14B)	366	668	343	106 (19)
H(14C)	209	613	369	101 (18)
H(15A)	497	503	126	72 (15)
H(15B)	578	437	155	71 (13)
H(15C)	586	555	208	67 (14)
H(17)	17	368	472	81 (15)
H(18)	52	453	646	66 (12)
H(19)	225	392	707	119 (21)
H(20)	358	237	586	112 (19)
H(21)	353	157	397	85 (18)
H(23)	315	−17	145	168 (28)
H(24)	250	−201	138	148 (30)
H(25)	60	−239	270	91 (22)
H(26)	−80	−100	407	182 (26)
H(27)	−30	80	415	232 (43)

Comparison of the Structures of 2a, 3b, 4, and 5. Structural relationships between the acetylide (**2a**, **3b**) and allenyl (**4**, **5**) clusters are illustrated in Figures 1–4 which also show the respective atomic numbering schemes. Although acetylenes and allenes are closely related and

Table V. A Selection of Important Bond Lengths (Å) and Angles (deg) for $Ru_3(CO)_6(\mu\text{-}CO)_2\{\mu_3\text{-}\eta^2\text{-}C{\equiv}C(t\text{-}Bu)\}(\mu\text{-}PPh_2)$ (3b)

(a) Bond Lengths

Ru(1)–Ru(2)	2.8151 (4)	Ru(1)–Ru(3)	2.8257 (4)	P–C(16)	1.822 (4)	P–C(22)	1.821 (4)
Ru(1)–P	2.337 (1)	Ru(1)–C(1)	1.918 (6)	C(1)–O(1)	1.128 (7)	C(2)–O(2)	1.121 (6)
Ru(1)–C(2)	1.892 (4)	Ru(1)–C(3)	2.060 (6)	C(3)–O(3)	1.150 (8)	C(4)–O(4)	1.128 (7)
Ru(1)–C(10)	2.046 (4)	Ru(2)–Ru(3)	2.7084 (5)	C(5)–O(5)	1.135 (6)	C(6)–O(6)	1.152 (6)
Ru(2)–C(3)	2.292 (6)	Ru(2)–C(4)	1.887 (6)	C(7)–O(7)	1.137 (6)	C(8)–O(8)	1.131 (6)
Ru(2)–C(5)	1.862 (5)	Ru(2)–C(6)	2.079 (5)	C(10)–C(11)	1.242 (5)	C(11)–C(12)	1.507 (6)
Ru(2)–C(10)	2.242 (4)	Ru(2)–C(11)	2.470 (4)	C(12)–C(13)	1.529 (6)	C(12)–C(14)	1.533 (9)
Ru(3)–P	2.337 (1)	Ru(3)–C(6)	2.161 (4)	C(12)–C(15)	1.530 (6)		
Ru(3)–C(7)	1.872 (5)	Ru(3)–C(8)	1.906 (4)				
Ru(3)–C(10)	2.315 (4)	Ru(3)–C(11)	2.398 (4)				

(b) Bond Angles

Ru(2)–Ru(1)–Ru(3)	57.39 (1)	Ru(2)–Ru(1)–P	109.32 (2)	P–Ru(3)–C(6)	161.7 (1)	P–Ru(3)–C(7)	98.2 (1)
Ru(2)–Ru(1)–C(1)	115.0 (1)	Ru(2)–Ru(1)–C(2)	135.6 (1)	P–Ru(3)–C(8)	100.9 (1)	P–Ru(3)–C(10)	73.4 (1)
Ru(2)–Ru(1)–C(3)	53.4 (1)	Ru(2)–Ru(1)–C(10)	52.0 (1)	P–Ru(3)–C(11)	95.0 (1)	C(6)–Ru(3)–C(7)	86.1 (1)
Ru(3)–Ru(1)–P	52.81 (2)	Ru(3)–Ru(1)–C(1)	106.1 (1)	C(6)–Ru(3)–C(8)	96.6 (1)	C(6)–Ru(3)–C(10)	93.1 (1)
Ru(3)–Ru(1)–C(2)	151.0 (1)	Ru(3)–Ru(1)–C(3)	110.1 (1)	C(6)–Ru(3)–C(11)	77.7 (1)	C(7)–Ru(3)–C(8)	93.1 (1)
Ru(3)–Ru(1)–C(10)	53.9 (1)	P–Ru(1)–C(1)	93.6 (1)	C(7)–Ru(3)–C(10)	146.0 (1)	C(7)–Ru(3)–C(11)	162.1 (1)
P–Ru(1)–C(2)	103.8 (1)	P–Ru(1)–C(3)	162.7 (1)	C(8)–Ru(3)–C(10)	120.7 (1)	C(8)–Ru(3)–C(11)	96.2 (1)
P–Ru(1)–C(10)	78.4 (1)	C(1)–Ru(1)–C(2)	90.9 (2)	C(10)–Ru(3)–C(11)	30.5 (1)		
C(1)–Ru(1)–C(3)	94.3 (2)	C(1)–Ru(1)–C(10)	159.3 (1)	Ru(1)–P–Ru(3)	74.40 (2)	Ru(1)–P–C(16)	117.4 (1)
C(2)–Ru(1)–C(3)	91.4 (2)	C(2)–Ru(1)–C(10)	109.5 (1)	Ru(1)–P–C(22)	120.0 (1)	Ru(3)–P–C(16)	116.8 (1)
C(3)–Ru(1)–C(10)	88.9 (1)	Ru(1)–Ru(2)–Ru(3)	61.50 (1)	Ru(3)–P–C(22)	124.5 (1)	C(16)–P–C(22)	103.0 (1)
Ru(1)–Ru(2)–C(3)	46.2 (1)	Ru(1)–Ru(2)–C(4)	133.4 (1)	Ru(1)–C(1)–O(1)	177.0 (2)	Ru(1)–C(2)–O(2)	178.6 (2)
Ru(1)–Ru(2)–C(5)	112.3 (1)	Ru(1)–Ru(2)–C(6)	111.9 (1)	Ru(1)–C(3)–Ru(2)	80.4 (1)	Ru(1)–C(3)–O(3)	149.3 (2)
Ru(1)–Ru(2)–C(10)	46.0 (1)	Ru(1)–Ru(2)–C(11)	75.0 (1)	Ru(2)–C(3)–O(3)	130.3 (2)	Ru(2)–C(4)–O(4)	178.2 (2)
Ru(3)–Ru(2)–C(3)	107.1 (1)	Ru(3)–Ru(2)–C(4)	145.3 (1)	Ru(2)–C(5)–O(5)	177.8 (2)	Ru(2)–C(6)–Ru(3)	79.4 (1)
Ru(3)–Ru(2)–C(5)	115.0 (1)	Ru(3)–Ru(2)–C(6)	51.7 (1)	Ru(2)–C(6)–O(6)	139.1 (1)	Ru(3)–C(6)–O(6)	140.9 (1)
Ru(3)–Ru(2)–C(10)	54.8 (1)	Ru(3)–Ru(2)–C(11)	54.9 (1)	Ru(3)–C(7)–O(7)	175.1 (2)	Ru(3)–C(8)–O(8)	178.1 (2)
C(3)–Ru(2)–C(4)	97.8 (2)	C(3)–Ru(2)–C(5)	87.2 (2)	Ru(1)–C(10)–Ru(2)	81.9 (1)	Ru(1)–C(10)–Ru(3)	80.5 (1)
C(3)–Ru(2)–C(6)	151.4 (1)	C(3)–Ru(2)–C(10)	78.7 (1)	Ru(1)–C(10)–C(11)	157.9 (1)	Ru(2)–C(10)–Ru(3)	72.9 (1)
C(3)–Ru(2)–C(11)	107.0 (1)	C(4)–Ru(2)–C(5)	89.4 (2)	Ru(2)–C(10)–C(11)	85.2 (1)	Ru(3)–C(10)–C(11)	78.5 (1)
C(4)–Ru(2)–C(6)	110.0 (2)	C(4)–Ru(2)–C(10)	109.3 (1)	Ru(2)–C(11)–Ru(3)	67.6 (1)	Ru(2)–C(11)–C(10)	64.7 (1)
C(4)–Ru(2)–C(11)	95.2 (1)	C(5)–Ru(2)–C(6)	86.7 (2)	Ru(2)–C(11)–C(12)	132.1 (1)	Ru(3)–C(11)–C(10)	71.0 (1)
C(5)–Ru(2)–C(10)	157.8 (1)	C(5)–Ru(2)–C(11)	164.2 (1)	Ru(3)–C(11)–C(12)	130.3 (1)	C(10)–C(11)–C(12)	154.3 (2)
C(6)–Ru(2)–C(10)	97.5 (1)	C(6)–Ru(2)–C(11)	77.6 (1)	C(11)–C(12)–C(13)	107.3 (2)	C(11)–C(12)–C(14)	107.4 (2)
C(10)–Ru(2)–C(11)	30.1 (1)	Ru(1)–Ru(3)–Ru(2)	61.11 (1)	C(11)–C(12)–C(15)	112.5 (2)	C(13)–C(12)–C(14)	109.9 (2)
Ru(1)–Ru(3)–P	52.79 (2)	Ru(1)–Ru(3)–C(6)	108.9 (1)	C(13)–C(12)–C(15)	110.4 (2)	C(14)–C(12)–C(15)	109.1 (2)
Ru(1)–Ru(3)–C(7)	102.8 (1)	Ru(1)–Ru(3)–C(8)	150.6 (1)				
Ru(1)–Ru(3)–C(10)	45.6 (1)	Ru(1)–Ru(3)–C(11)	75.9 (1)				
Ru(2)–Ru(3)–P	112.96 (2)	Ru(2)–Ru(3)–C(6)	49.0 (1)				
Ru(2)–Ru(3)–C(7)	105.9 (1)	Ru(2)–Ru(3)–C(8)	137.7 (1)				
Ru(2)–Ru(3)–C(10)	52.3 (1)	Ru(2)–Ru(3)–C(11)	57.5 (1)				

their coordination chemistries show some resemblance,[22] there are to our knowledge no known examples of the conversion of a μ_3-acetylide to a μ_3-allenyl unit on the face of a trinuclear cluster by addition of a carbene unit.[23] The series of structures reported herein therefore provide a unique opportunity to compare bonding modes for two hydrocarbyls having the same donor capacity on a similar metal framework.

In three of the four structures (**3b**, **4**, **5**) metal–metal bonds define the edges of an equilateral ruthenium triangle with Ru–Ru bond lengths (2.6653 (6)–3.0965 (7)Å) lying within the normal range. The Ru(1)–Ru(3) distance in **2a** (3.466 (1) Å) is distinctly longer and indicative of the absence of a direct metal–metal interaction in this case. These results are consistent with electron counts of 48e for the "closed" clusters **3b**, **4**, and **5** and 50e for the "open" triangular framework of **2a**.

There are significant differences between the nature and orientation of the phosphido bridges in **2a** when compared to those of **3b**, **4**, and **5**. In the latter three clusters the Ru–P bond lengths (average: 2.337 Å in **3b**; 2.337 Å in **4**; 2.333 Å in **5**) are identical, the angles subtended at phosphorus are acute (Ru–P–Ru = 74.4 (0)° in **3b**, 74.3 (0)°, in **4**, and 71.9 (1)° in **5**), and the phosphorus atom occupies *equatorial* sites on two ruthenium atoms, lying approximately in the same plane as the three ruthenium atoms.[24] In **2a** however the phosphido group has an *axial* configuration with respect to the Ru_3 plane (Figure 1). It might reasonably be argued that steric interactions between the phenyl rings on the phosphido bridge and the methyl groups of the isopropyl substituent on the acetylide force an axial configuration for the PPh_2 groups in **2a** whereas the absence of such interactions in **3b**, **4**, and **5** allows the phosphorus atom to adopt equatorial coordination sites. Furthermore, the disposition of the acetylide

---

[22] (a) Bowden, F. L.; Giles, R. *Coord. Chem. Rev.* **1976**, *20*, 81. (b) Jacobs, T. L. *The Chemistry of Allenes*; London, S. R., Ed.; Academic: Toronto, 1982; Vol. 2, p 277. (c) Shaw, B. L.; Stringer, A. J. *Inorg. Chim. Acta Rev.* **1973**, *7*, 1. (d) Otsuka, S.; Nakamura, A. *Adv. Organomet. Chem.* **1976**, *14*, 245.

[23] Triruthenium and triosmium acetylide clusters derived from 1-(dimethylamino)but-2-yne ($HC{\equiv}CCH_2NMe_2$) undergo isomerizations which are related to the acetylide–allenyl transformation of **2** to **6**. See: Aime, S.; Osella, D.; Arce, A. J.; Deeming, A. J.; Hursthouse, M. B.; Galas, A. M. R. *J. Chem. Soc., Dalton Trans.* **1984**, 1981. Aime, S.; Jannon, G.; Osella, D.; Arce, A. J.; Demming, A. J. *J. Chem. Soc., Dalton Trans.* **1987**, 1984.

[24] Dihedral angles between the planes Ru(1), Ru(2), Ru(3) and Ru(1), P, Ru(3) are as follows: **2a**, 120.91°; **3b**, 11.92; **4**, 9.83°; **5**, 8.46°.

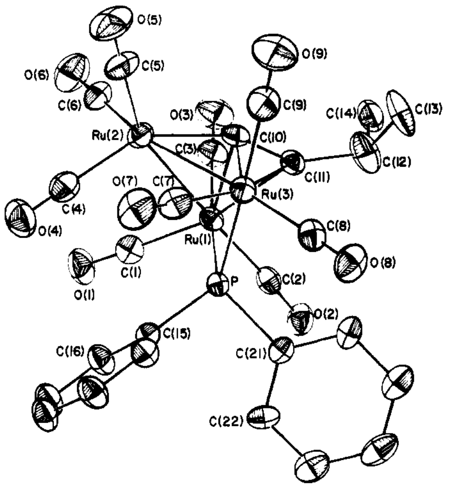

Figure 1. An ORTEP II plot of the molecular structure of $Ru_3(CO)_9\{\mu_3\text{-}\eta^2\text{-}C{\equiv}C(i\text{-}Pr)\}(\mu\text{-}PPh_2)$ (**2a**) showing the atomic numbering.

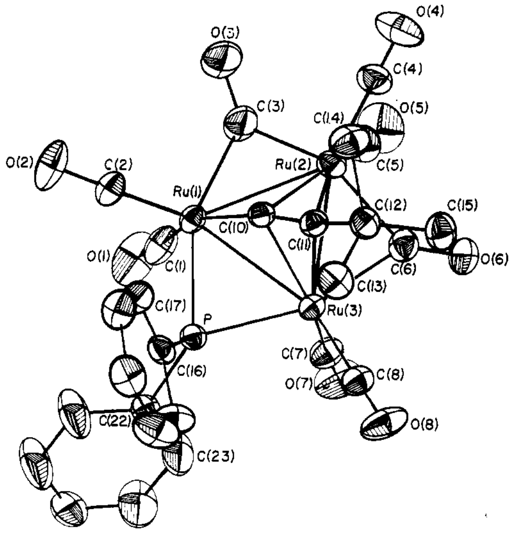

Figure 2. The structure of $Ru_3(CO)_6(\mu\text{-}CO)_2\{\mu_3\text{-}\eta^2\text{-}C{\equiv}C(t\text{-}Bu)\}(\mu\text{-}PPh_2)$ (**3b**) drawn to illustrate the relationship of phosphido and acetylide ligands.

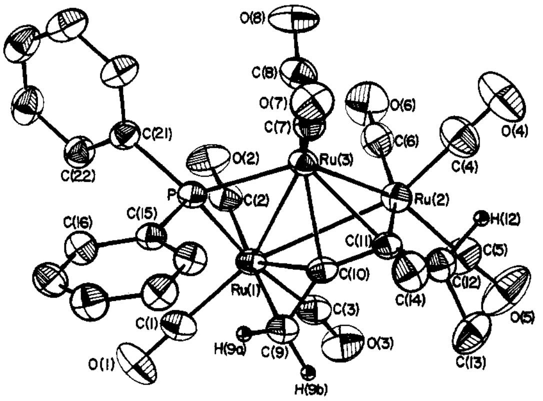

Figure 3. A perspective view of the structure of $Ru_3(CO)_8\{\mu_3\text{-}\eta^3\text{-}CH_2{=}C{=}C(i\text{-}Pr)\}(\mu\text{-}PPh_2)$ (**4**). The Ru_3C_2 skeletal framework is illustrated.

Table VI. Atomic Coordinates (Fractional ×10^4) and Hydrogen Atom Thermal Parameters for $Ru_3(CO)_8\{\mu_3\text{-}\eta^3\text{-}CH_2CC(i\text{-}Pr)\}(\mu\text{-}PPh_2)$ (4)

(a) Heavy Atoms

atom	x	y	z
Ru(1)	2223.3 (4)	1899.0 (4)	2419.5 (2)
Ru(2)	1483.6 (4)	1187.0 (4)	3835.9 (3)
Ru(3)	2910.1 (4)	−5.8 (4)	3145.6 (2)
P	3272.0 (12)	328.3 (12)	2053.1 (8)
O(1)	2660 (5)	3392 (5)	1224 (3)
O(2)	35 (4)	950 (4)	1794 (3)
O(3)	1005 (5)	3814 (4)	3073 (3)
O(4)	1448 (6)	−416 (6)	4990 (4)
O(5)	921 (5)	3058 (6)	4758 (4)
O(6)	−888 (4)	446 (6)	3306 (3)
O(7)	4682 (4)	−1674 (4)	3548 (3)
O(8)	1123 (4)	−1773 (4)	2954 (3)
C(1)	2501 (5)	2829 (5)	1658 (4)
C(2)	846 (5)	1281 (5)	2041 (3)
C(3)	1448 (5)	3054 (5)	2885 (3)
C(4)	1467 (6)	209 (7)	4538 (4)
C(5)	1091 (5)	2377 (6)	4380 (4)
C(6)	−20 (6)	742 (6)	3496 (4)
C(7)	3998 (5)	−1039 (5)	3402 (3)
C(8)	1790 (6)	−1108 (6)	3035 (4)
C(9)	3910 (5)	2452 (5)	2903 (3)
C(10)	3533 (4)	1613 (4)	3307 (3)
C(11)	3184 (5)	1376 (4)	3932 (3)
C(12)	3992 (5)	1444 (5)	4561 (3)
C(13)	4028 (9)	2625 (8)	4810 (5)
C(14)	5189 (6)	1100 (8)	4424 (4)
C(15)	4725 (4)	473 (4)	1806 (3)
C(16)	4980 (5)	521 (6)	1128 (3)
C(17)	6067 (6)	639 (6)	947 (4)
C(18)	6920 (6)	737 (6)	1434 (4)
C(19)	6701 (5)	695 (6)	2108 (4)
C(20)	5606 (5)	558 (5)	2291 (3)
C(21)	2644 (5)	−508 (5)	1363 (3)
C(22)	2072 (5)	−42 (6)	808 (3)
C(23)	1627 (6)	−697 (7)	281 (4)
C(24)	1748 (6)	−1796 (7)	314 (4)
C(25)	2306 (6)	−2279 (6)	860 (5)
C(26)	2762 (6)	−1622 (6)	1389 (4)

(b) Hydrogen Atoms

atom	x	y	z	U_{iso}, Å^2
H(9A)	440 (4)	231 (4)	258 (2)	47 (13)
H(9B)	392 (4)	318 (4)	312 (2)	57 (15)
H(12)	364 (4)	83 (4)	496 (2)	44 (13)
H(13A)	451 (6)	261 (5)	519 (3)	68 (22)
H(13B)	437 (6)	298 (7)	444 (4)	97 (29)
H(13C)	334 (7)	277 (7)	490 (4)	118 (32)
H(14A)	554 (5)	147 (5)	399 (3)	76 (20)
H(14B)	566 (4)	116 (4)	489 (3)	75 (16)
H(14C)	515 (6)	29 (6)	423 (3)	92 (23)
H(16)	441 (4)	51 (4)	81 (3)	43 (16)
H(17)	626 (5)	65 (5)	46 (3)	97 (22)
H(18)	763 (4)	81 (4)	136 (3)	75 (16)
H(19)	729 (5)	70 (5)	239 (3)	74 (18)
H(20)	549 (4)	46 (4)	275 (2)	51 (15)
H(22)	193 (5)	70 (5)	77 (3)	57 (20)
H(23)	116 (6)	−24 (6)	−7 (4)	69 (27)
H(24)	140 (6)	−226 (6)	−7 (4)	98 (25)
H(25)	253 (6)	−298 (7)	84 (4)	104 (28)
H(26)	317 (4)	−195 (4)	174 (2)	36 (14)

relative to the phosphido bridge is quite different in **2a** and **3b**. The two are related by a 120° twist of the acetylide. A visual examination of the ORTEP plot of **3b** (Figure 2) shows that a 120° clockwise shift of the acetylide will result in severe steric interactions between the *tert*-butyl methyl group and an equatorial *P*-phenyl group. Thus decarbonylation of **2a** appears to generate a cluster preferring the phosphido bridge in equatorial sites, but in order to do so the acetylide ligand must rearrange so as to avoid steric interactions with the μ-PPh_2 group. Whether or not a dynamic equilibrium exists between axial and equatorial phosphido bridged forms of **2a** and **3b**

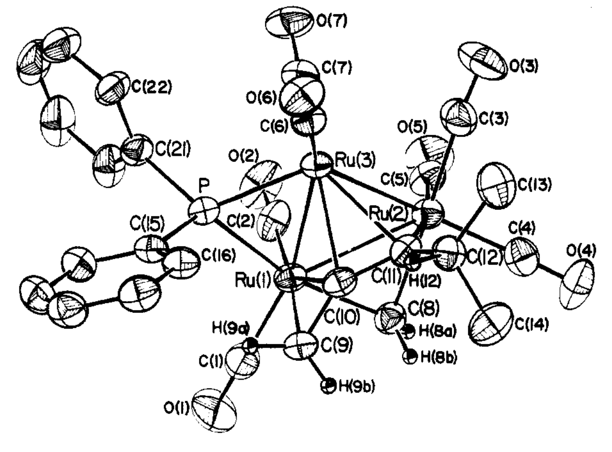

Figure 4. A view of $Ru_3(CO)_7(\mu-CH_2)\{\mu_3-\eta^3-CH_2{=}C{=}C(i-Pr)\}(\mu-PPh_2)$ (**5**) similar to that of **4**.

Scheme I

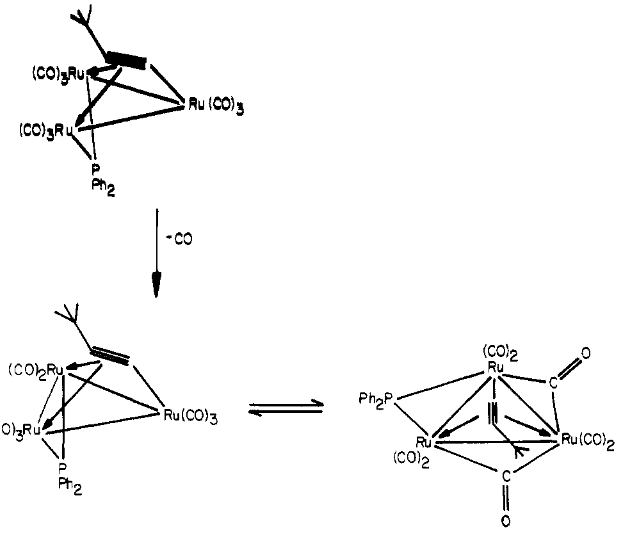

Table VII. Important Bond Lengths (Å) and Angles for $Ru_3(CO)_8\{\mu_3-\eta^3-CH_2CC(i-Pr)\}(\mu-PPh_2)$ (4)

(a) Bond Lengths

Ru(1)–Ru(2)	3.0965 (7)	Ru(1)–Ru(3)	2.8252 (6)
Ru(2)–Ru(3)	2.6653 (6)	Ru(1)–P	2.419 (2)
Ru(3)–P	2.255 (2)	Ru(1)–C(1)	1.923 (7)
Ru(1)–C(2)	1.916 (6)	Ru(1)–C(3)	1.942 (6)
Ru(2)–C(4)	1.828 (9)	Ru(2)–C(5)	1.879 (8)
Ru(2)–C(6)	1.951 (7)	Ru(3)–C(7)	1.856 (6)
Ru(3)–C(8)	1.897 (7)	Ru(1)–C(9)	2.274 (6)
Ru(1)–C(10)	2.301 (5)	Ru(2)–C(11)	2.033 (6)
Ru(3)–C(10)	2.127 (5)	Ru(3)–C(11)	2.299 (5)
P–C(15)	1.830 (6)	P–C(21)	1.826 (6)
C(1)–O(1)	1.121 (9)	C(2)–O(2)	1.130 (8)
C(3)–O(3)	1.140 (8)	C(4)–O(4)	1.173 (11)
C(5)–O(5)	1.141 (11)	C(6)–O(6)	1.137 (9)
C(7)–O(7)	1.148 (8)	C(8)–O(8)	1.140 (9)
C(9)–C(10)	1.386 (8)	C(10)–C(11)	1.352 (8)
C(11)–C(12)	1.528 (8)	C(12)–C(13)	1.521 (12)
C(12)–C(14)	1.523 (10)		

(b) Bond Angles

Ru(2)–Ru(1)–Ru(3)	53.26 (1)	Ru(2)–Ru(1)–P	102.94 (3)
Ru(2)–Ru(1)–C(1)	159.7 (2)	Ru(2)–Ru(1)–C(2)	87.7 (1)
Ru(2)–Ru(1)–C(3)	67.1 (1)	Ru(2)–Ru(1)–C(9)	89.7 (1)
Ru(2)–Ru(1)–C(10)	59.2 (1)	Ru(3)–Ru(1)–P	50.22 (3)
Ru(3)–Ru(1)–C(1)	145.3 (2)	Ru(3)–Ru(1)–C(2)	95.1 (1)
Ru(3)–Ru(1)–C(3)	119.3 (1)	Ru(3)–Ru(1)–C(9)	79.0 (1)
Ru(3)–Ru(1)–C(10)	47.7 (1)	P–Ru(1)–C(1)	96.9 (2)
P–Ru(1)–C(2)	90.9 (1)	P–Ru(1)–C(3)	169.2 (1)
P–Ru(1)–C(9)	84.4 (1)	P–Ru(1)–C(10)	76.6 (1)
C(1)–Ru(1)–C(2)	96.3 (2)	C(1)–Ru(1)–C(3)	92.7 (2)
C(1)–Ru(1)–C(9)	88.0 (2)	C(1)–Ru(1)–C(10)	122.9 (2)
C(2)–Ru(1)–C(3)	92.9 (22)	C(2)–Ru(1)–C(9)	174.0 (2)
C(2)–Ru(1–C(10)	139.7 (2)	C(3)–Ru(1)–C(9)	91.0 (2)
C(3)–Ru(1)–C(10)	94.0 (2)	C(9)–Ru(1)–C(10)	35.2 (2)
Ru(1)–Ru(2)–Ru(3)	58.15 (1)	Ru(1)–Ru(2)–C(4)	151.7 (2)
Ru(1)–Ru(2)–C(5)	112.9 (2)	Ru(1)–Ru(2)–C(6)	94.0 (2)
Ru(1)–Ru(2)–C(11)	73.8 (1)	Ru(3)–Ru(2)–C(4)	93.7 (2)
Ru(3)–Ru(2)–C(5)	154.0 (2)	Ru(3)–Ru(2)–C(6)	105.7 (2)
Ru(3)–Ru(2)–C(11)	56.7 (11)	C(4)–Ru(2)–C(5)	93.4 (3)
C(4)–Ru(2)–C(6)	91.7 (3)	C(4)–Ru(2)–C(11)	93.3 (3)
C(5)–Ru(2)–C(6)	99.1 (3)	C(5)–Ru(2)–C(11)	97.9 (2)
C(6)–Ru(2)–C(11)	162.0 (2)	Ru(1)–Ru(3)–Ru(2)	68.59 (1)
Ru(1)–Ru(3)–P	55.49 (3)	Ru(1)–Ru(3)–C(7)	150.9 (1)
Ru(1)–Ru(3)–C(8)	110.1 (2)	Ru(1)–Ru(3)–C(10)	53.1 (1)
Ru(1)–Ru(3)–C(11)	76.3 (1)	Ru(2)–Ru(3)–P	123.31 (3)
Ru(2)–Ru(3)–C(7)	133.3 (1)	Ru(2)–Ru(3)–C(8)	89.0 (2)
Ru(2)–Ru(3)–C(10)	69.1 (1)	Ru(2)–Ru(3)–C(11)	47.6 (1)
P–Ru(3)–C(7)	102.4 (1)	P–Ru(3)–C(8)	100.9 (2)
P–Ru(3)–C(10)	83.7 (1)	P–Ru(3)–C(11)	118.9 (1)
C(7)–Ru(3)–C(8)	91.4 (2)	C(7)–Ru(3)–C(10)	111.0 (2)
C(7)–Ru(3)–C(11)	104.2 (2)	C(8)–Ru(3)–C(10)	155.8 (2)
C(8)–Ru(3)–C(11)	132.0 (2)	C(10)–Ru(3)–C(11)	35.3 (1)
Ru(1)–P–Ru(3)	74.29 (3)	Ru(1)–P–C(15)	120.9 (1)
Ru(1)–P–C(21)	117.9 (1)	Ru(3)–P–C(15)	120.3 (1)
Ru(3)–P–C(21)	121.2 (1)	C(15)–P–C(21)	102.1 (2)
Ru(1)–C(1)–O(1)	178.4 (2)	Ru(1)–C(2)–O(2)	176.8 (2)
Ru(1)–C(3)–O(3)	170.1 (2)	Ru(2)–C(4)–O(4)	179.5 (3)
Ru(2)–C(5)–O(5)	173.4 (3)	Ru(2)–C(6)–O(6)	177.5 (3)
Ru(3)–C(7)–O(7)	178.6 (2)	Ru(3)–C(8)–O(8)	178.5 (2)
Ru(1)–C(9)–C(10)	73.4 (2)	Ru(1)–C(10)–Ru(3)	79.2 (2)
Ru(1)–C(10)–C(9)	71.3 (2)	Ru(1)–C(10)–C(11)	119.6 (2)
Ru(3)–C(10)–C(9)	136.2 (2)	Ru(3)–C(10)–C(11)	79.3 (2)
C(9)–C(10)–C(11)	143.7 (3)	Ru(2)–C(11)–Ru(3)	75.7 (2)
Ru(2)–C(11)–C(10)	107.1 (2)	Ru(2)–C(11)–C(12)	131.2 (2)
Ru(3)–C(11)–C(10)	65.4 (2)	Ru(3)–C(11)–C(12)	130.2 (2)
C(10)–C(11)–C(12)	121.1 (3)	C(11)–C(12)–C(13)	108.5 (4)
C(11)–C(12)–C(14)	113.1 (3)	C(13)–C(12)–C(14)	108.0 (4)

which involve acetylide migration remains to be determined. The type of process which can be envisioned is shown in Scheme I and would provide a link between the stereochemistry of **2a** and **3b**, **4**, or **5**.

The acetylide ligand in **2a** and **3b** is σ-bonded to one ruthenium atom (Ru(2)–C(10) = 1.960 (6) Å in **2a**: Ru(1)–C(10) = 2.046 (4) Å in **3b**) and η-coordinated to the remaining metal atoms. Comparison with other μ-η-bound alkynyl ligands (Table X) elicits the following comments: (i) Ru–acetylide σ-bonds produce shorter Ru–C distances than η-interactions via the acetylide π-orbitals. (ii) In both **2a** and **3b** the triple bond is lengthened substantially over the value in free acetylene (1.201 (1) Å).[25] Generally for μ-η-acetylides the $-C{\equiv}C-$ bond length increases as the number of interacting metals increases (Table X), but there are exceptions to the correlation. (iii) Bend back angles at the β-carbon atom may provide a better estimate of the extent of perturbation of the acetylide. In **2a** and **3b** the $-C{\equiv}C-$ distance (1.284 (8) Å in **2a**: 1.242 (5) Å in **3b**) and the C(10)–C(11)–C(12) (145.2 (3)° in **2a**; 154.3 (2)° in **3b**) and Ru–C(10)–C(11) (Ru(2)–C(10)–C(11) = 154.0 (2)° in **2a**; Ru(1)–C(10)—C(11) = 157.9 (1)° in **3b**) angles indicate that the acetylides have undergone a significant distortion from linearity toward a relative trans disposition of the σ-bound metal and the acetylide substituent. (iv) The C(10) carbon atom in both structures is exposed, much like the carbide carbon atom in M_4 cluster carbides.

---

[25] Kennard, O.; Watson, D. G.; Allen, F. H.; Isaccs, N. W.; Motherwell, W. D. S.; Petterson, R. C.; Town, W. G., Eds.; *Molecular Structures and Dimensions*; Oosthoek, N. V. A., Ed.; Utrecht, 1976; Vol. A1.

Table VIII. Atomic Coordinates (Fractional ×10⁴) and Hydrogen Atom Thermal Parameters for $Ru_3(CO)_7(\mu\text{-}CH_2)\{\mu_3\text{-}\eta^3\text{-}CH_2CC(i\text{-}Pr)\}(\mu\text{-}PPh_2)$ (5)

(a) Heavy Atoms

atom	*x*	*y*	*z*
Ru(1)	2128.4 (5)	1876.9 (5)	2507.1 (3)
Ru(2)	1308.9 (4)	1337.7 (5)	1214.8 (3)
Ru(3)	2835.5 (4)	−1.6 (4)	1844.9 (3)
P	3262.9 (15)	399.0 (15)	2947.5 (9)
O(1)	2226 (9)	3803 (6)	3508 (4)
O(2)	19 (5)	889 (6)	3113 (3)
O(3)	912 (6)	−845 (6)	462 (4)
O(4)	860 (5)	2821 (6)	−8 (3)
O(5)	−1142 (5)	1064 (6)	1682 (4)
O(6)	4685 (5)	−1554 (5)	1404 (3)
O(7)	1268 (5)	−1882 (5)	2209 (3)
C(1)	2185 (8)	3083 (7)	3133 (4)
C(2)	802 (6)	1276 (7)	2878 (4)
C(3)	1146 (7)	−72 (8)	761 (4)
C(4)	1006 (6)	2265 (7)	444 (4)
C(5)	−247 (6)	1164 (7)	1526 (4)
C(6)	3969 (6)	−986 (6)	1557 (4)
C(7)	1864 (6)	−1186 (6)	2067 (4)
C(8)	1324 (7)	2897 (6)	1789 (4)
C(9)	3862 (6)	2538 (6)	2120 (4)
C(10)	3463 (5)	1711 (5)	1703 (3)
C(11)	3061 (6)	1444 (6)	1087 (3)
C(12)	3818 (6)	1373 (6)	476 (4)
C(13)	3454 (9)	496 (10)	−41 (5)
C(14)	3932 (10)	2534 (10)	177 (6)
C(15)	4746 (5)	531 (5)	3179 (3)
C(16)	5596 (6)	603 (6)	2716 (4)
C(17)	6687 (6)	733 (7)	2928 (5)
C(18)	6966 (7)	777 (8)	3599 (5)
C(19)	6135 (8)	703 (8)	4065 (5)
C(20)	5035 (7)	575 (7)	3863 (4)
C(21)	2761 (6)	−547 (6)	3612 (4)
C(22)	3169 (8)	−1654 (7)	3624 (5)
C(23)	2775 (11)	−2318 (9)	4150 (6)
C(24)	2045 (11)	−1939 (12)	4622 (6)
C(25)	1676 (8)	−894 (13)	4602 (5)
C(26)	2035 (7)	−185 (9)	4097 (4)

(b) Hydrogen Atoms

atom	*x*	*y*	*z*	U_{iso}, Å^2
H(8A)	59 (5)	325 (5)	186 (3)	48 (15)
H(8B)	183 (6)	342 (6)	157 (3)	71 (20)
H(9A)	431 (5)	236 (5)	249 (3)	34 (16)
H(9B)	383 (6)	319 (6)	194 (3)	70 (22)
H(12)	480 (4)	120 (4)	62 (3)	54 (14)
H(13A)	391 (7)	51 (7)	−42 (4)	76 (27)
H(13B)	267 (8)	81 (8)	−24 (5)	129 (33)
H(13C)	334 (8)	−50 (9)	27 (5)	136 (33)
H(14A)	457 (8)	242 (8)	−19 (5)	161 (37)
H(14B)	317 (7)	274 (7)	−1 (4)	82 (28)
H(14C)	424 (8)	307 (9)	57 (5)	139 (37)
H(16)	541 (5)	55 (6)	222 (3)	57 (20)
H(17)	712 (6)	80 (6)	263 (3)	67 (22)
H(18)	763 (6)	91 (6)	367 (3)	79 (23)
H(19)	632 (6)	69 (7)	444 (4)	86 (28)
H(20)	454 (6)	56 (6)	417 (3)	57 (22)
H(22)	367 (7)	−183 (7)	341 (5)	90 (31)
H(23)	316 (7)	−308 (8)	406 (5)	108 (33)
H(24)	187 (7)	−247 (8)	495 (4)	146 (32)
H(25)	117 (8)	−72 (8)	482 (5)	99 (37)
H(26)	181 (7)	46 (8)	402 (4)	71 (32)

Table IX. Important Bond Lengths (Å) and Angles (deg) for $Ru_3(CO)_7(\mu\text{-}CH_2)\{\mu_3\text{-}\eta^3\text{-}CH_2CC(i\text{-}Pr)\}(\mu\text{-}PPh_2)$ (5)

(a) Bond Lengths

Ru(1)–Ru(2)	2.7971 (8)	Ru(1)–Ru(3)	2.7326 (7)
Ru(2)–Ru(3)	2.7197 (7)	Ru(1)–P	2.387 (2)
Ru(3)–P	2.278 (2)	Ru(1)–C(1)	1.899 (9)
Ru(1)–C(2)	1.882 (8)	Ru(2)–C(3)	1.919 (9)
Ru(2)–C(4)	1.913 (8)	Ru(2)–C(5)	1.961 (7)
Ru(3)–C(6)	1.880 (7)	Ru(3)–C(7)	1.881 (7)
Ru(1)–C(8)	2.097 (8)	Ru(2)–C(8)	2.181 (7)
Ru(1)–C(9)	2.337 (7)	Ru(1)–C(10)	2.253 (6)
Ru(3)–C(10)	2.200 (6)	Ru(2)–C(11)	2.103 (7)
Ru(3)–C(11)	2.300 (7)	P–C(15)	1.832 (6)
P–C(21)	1.830 (7)	C(1)–O(1)	1.135 (12)
C(2)–O(2)	1.139 (10)	C(3)–O(3)	1.132 (11)
C(4)–O(4)	1.125 (11)	C(5)–O(5)	1.115 (9)
C(6)–O(6)	1.131 (9)	C(7)–O(7)	1.129 (9)
C(9)–C(10)	1.371 (10)	C(10)–C(11)	1.340 (9)
C(11)–C(12)	1.506 (10)	C(12)–C(13)	1.524 (13)
C(12)–C(14)	1.515 (14)	C(8)···C(9)	2.919 (10)

(b) Bond Angles

Ru(2)–Ru(1)–Ru(3)	58.91 (1)	Ru(2)–Ru(1)–P	110.77 (4)
Ru(2)–Ru(1)–C(1)	141.0 (2)	Ru(2)–Ru(1)–C(2)	88.5 (2)
Ru(2)–Ru(1)–C(8)	50.5 (2)	Ru(2)–Ru(1)–C(9)	95.1 (1)
Ru(2)–Ru(1)–C(10)	65.6 (1)	Ru(3)–Ru(1)–P	52.32 (4)
Ru(3)–Ru(1)–C(1)	157.6 (2)	Ru(3)–Ru(1)–C(2)	97.4 (2)
Ru(3)–Ru(1)–C(8)	107.3 (2)	Ru(3)–Ru(1)–C(9)	81.4 (1)
Ru(3)–Ru(1)–C(10)	51.3 (1)	P–Ru(1)–C(1)	108.0 (2)
P–Ru(1)–C(2)	92.8 (2)	P–Ru(1)–C(8)	158.9 (2)
P–Ru(1)–C(9)	82.6 (1)	P–Ru(1)–C(10)	77.9 (1)
C(1)–Ru(1)–C(2)	93.9 (3)	C(1)–Ru(1)–C(8)	90.6 (3)
C(1)–Ru(1)–C(9)	85.6 (3)	C(1)–Ru(1)–C(10)	119.9 (3)
C(2)–Ru(1)–C(8)	95.8 (3)	C(2)–Ru(1)–C(9)	175.0 (3)
C(2)–Ru(1)–C(10)	146.2 (2)	C(8)–Ru(1)–C(9)	89.2 (2)
C(8)–Ru(1)–C(10)	84.2 (2)	C(9)–Ru(1)–C(10)	34.7 (2)
Ru(1)–Ru(2)–Ru(3)	59.37 (1)	Ru(1)–Ru(2)–C(3)	131.4 (2)
Ru(1)–Ru(2)–C(4)	130.7 (2)	Ru(1)–Ru(2)–C(5)	93.9 (2)
Ru(1)–Ru(2)–C(8)	47.9 (2)	Ru(1)–Ru(2)–C(11)	75.6 (1)
Ru(3)–Ru(2)–C(3)	76.1 (2)	Ru(3)–Ru(2)–C(4)	145.9 (2)
Ru(3)–Ru(2)–C(5)	115.1 (2)	Ru(3)–Ru(2)–C(8)	105.3 (2)
Ru(3)–Ru(2)–C(11)	55.2 (1)	C(3)–Ru(2)–C(4)	97.0 (3)
C(3)–Ru(2)–C(5)	87.6 (3)	C(3)–Ru(2)–C(8)	173.7 (3)
C(3)–Ru(2)–C(11)	95.6 (3)	C(4)–Ru(2)–C(5)	97.6 (3)
C(4)–Ru(2)–C(8)	85.2 (3)	C(4)–Ru(2)–C(11)	93.2 (3)
C(5)–Ru(2)–C(8)	86.3 (3)	C(5)–Ru(2)–C(11)	168.3 (2)
C(8)–Ru(2)–C(11)	90.2 (2)	Ru(1)–Ru(3)–Ru(2)	61.73 (1)
Ru(1)–Ru(3)–P	56.01 (4)	Ru(1)–Ru(3)–C(6)	151.9 (2)
Ru(1)–Ru(3)–C(7)	108.7 (2)	Ru(1)–Ru(3)–C(10)	53.0 (1)
Ru(1)–Ru(3)–C(11)	74.1 (1)	Ru(2)–Ru(3)–P	117.23 (4)
Ru(2)–Ru(3)–C(6)	135.3 (2)	Ru(2)–Ru(3)–C(7)	98.1 (2)
Ru(2)–Ru(3)–C(10)	67.6 (1)	Ru(2)–Ru(3)–C(11)	48.7 (1)
P–Ru(3)–C(6)	105.1 (2)	P–Ru(3)–C(7)	94.2 (2)
P–Ru(3)–C(10)	81.4 (1)	P–Ru(3)–C(11)	115.6 (1)
C(6)–Ru(3)–C(7)	92.2 (3)	C(6)–Ru(3)–C(10)	107.6 (2)
C(6)–Ru(3)–C(11)	101.1 (2)	C(7)–Ru(3)–C(10)	160.2 (2)
C(7)–Ru(3)–C(11)	142.2 (2)	C(10)–Ru(3)–C(11)	34.6 (2)
Ru(1)–P–Ru(3)	71.67 (4)	Ru(1)–P–C(15)	125.0 (2)
Ru(1)–P–C(21)	122.2 (2)	Ru(3)–P–C(15)	118.5 (2)
Ru(3)–P–C(21)	118.5 (2)	C(15)–P–C(21)	100.6 (3)
Ru(1)–C(1)–O(1)	179.6 (4)	Ru(1)–C(2)–O(2)	177.8 (3)
Ru(2)–C(3)–O(3)	170.5 (3)	Ru(2)–C(4)–O(4)	178.0 (3)
Ru(2)–C(5)–O(5)	177.7 (3)	Ru(3)–C(6)–O(6)	176.8 (2)
Ru(3)–C(7)–O(7)	178.6 (3)	Ru(1)–C(8)–Ru(2)	81.6 (1)
Ru(1)–C(9)–C(10)	69.3 (2)	Ru(1)–C(10)–Ru(3)	75.7 (1)
Ru(1)–C(10)–C(9)	76.0 (3)	Ru(1)–C(10)–C(11)	113.9 (2)
Ru(3)–C(10)–C(9)	135.6 (3)	Ru(3)–C(10)–C(11)	76.8 (2)
C(9)–C(10)–C(11)	146.8 (4)	Ru(2)–C(11)–Ru(3)	76.1 (1)
Ru(2)–C(11)–C(10)	105.0 (2)	Ru(2)–C(11)–C(12)	133.3 (2)
Ru(3)–C(11)–C(10)	68.6 (2)	Ru(3)–C(11)–C(12)	123.1 (2)
C(10)–C(11)–C(12)	121.5 (3)	C(11)–C(12)–C(13)	113.7 (4)
C(11)–C(12)–C(14)	108.2 (5)	C(13)–C(12)–C(14)	113.6 (6)

The resulting attachment of the methylene group to C_α of the acetylide in **3b** results in conversion of the acetylide into an allenyl fragment in **4** where bond lengths and π-interactions with the metal atoms suggest C(9)–C(10) and C(10)–C(11) double bonds. The bending of the allenyl fragment at C(10) with an angle C(9)–C(10)–C(11) of 143.7 (3)° is a common feature of π-coordinated allenyl fragments[22,23] and can be compared with a corresponding angle of 142.3 (6)° in the cluster $(\mu\text{-H})Ru_3(CO)_9(\mu_3\text{-}\eta^3\text{-Me(H)-C{=}C{=}CEt})$.[26] Indeed the hydrocarbyl–metal interactions in **4** and the resulting ligand stereochemistry bear a rather remarkable resemblance to the methylethylallenyl cluster.[26]

Table X. A Comparison of Structural Parameters for Some μ-η-Bound Acetylides in Ruthenium Complexes

	bond lengths, Å				bend back angles, deg		
compd	–C≡C–	Ru–C(σ)	M–C$_\alpha$(π)	M–C$_\beta$(π)	C$_\alpha$	C$_\beta$	ref
(a) μ-η^2							
Ru$_2$(CO)$_6${μ-η^2-C≡C(*t*-Bu)}(μ-PPh$_2$)	1.218 (4)	2.044 (3)	2.285 (3)	2.417 (3)	21.1 (1)	21.5 (1)	1b, 11
Ru$_2$(CO)$_5${μ-η^2-C≡C(*i*-Pr)}(μ-PPh$_2$){Ph$_2$PC≡C(*i*-Pr)}	1.234 (5)	2.034 (4)	2.280 (3)	2.406 (4)	20.1 (1)	21.2 (2)	1b, 32
Ru$_3$(CO)$_6${μ-η^2-C≡C(*t*-Bu)}{μ-C≡C(*t*-Bu)}{Ph$_2$PC≡C(*t*-Bu)}	1.239 (13)	2.046 (9)	2.323 (9)	2.422 (9)	11.2 (4)	20.2 (5)	33
Ru$_4$(CO)$_{13}${μ-η^2-C≡C(*t*-Bu)}(μ-PPh$_2$)	1.199 (12)	2.044 (8)	2.285 (8)	2.509 (8)	4.7 (4)	20.2 (5)	34
Ru$_4$(CO)$_8${μ-η^2-C≡C(*t*-Bu)}{μ_3-η^2-C≡C(*t*-Bu)}(μ-PPh$_2$)$_2$-{Ph$_2$PC≡C(*t*-Bu)}	1.228 (11)	2.041 (7)	2.292 (11)	2.620 (7)	6.5 (3)	16.7 (4)	34
(b) μ_3-η^2							
(μ-H)Ru$_3$(CO)$_9${μ_3-η^2-C≡C(*t*-Bu)}	1.315 (3)	1.947 (3)	2.207 (3)	2.268 (3)	26.3 (2)	39.0 (2)	19
			2.214 (3)	2.711 (3)			
Hg[Ru$_3$(CO)$_9${μ_3-η^2-C≡C(*t*-Bu)}]$_2$	1.32 (4)	1.98 (3)	2.20 (3)	2.31 (4)	24 (3)	37 (3)	35
	1.27 (4)	1.96 (3)	2.16 (3)	2.27 (4)			
			2.17 (3)	2.24 (3)			
			2.14 (3)	2.21 (3)	24 (3)	37 (3)	
Ru$_3$(CO)$_9${μ_3-η^2-C≡C(*i*-Pr)}(μ-PPh$_2$)	1.284	1.960 (5)	2.259 (5)	2.381 (5)	26.0 (2)	34.8 (2)	this work
			2.262 (5)	2.381 (5)			
Ru$_3$(CO)$_6$(μ-CO)$_2${μ_3-η^2-C≡C(*t*-Bu)}(μ-PPh$_2$)	1.242 (5)	2.046 (4)	2.315 (4)	2.398 (4)	22.1 (1)	25.7 (2)	this work
			2.243 (3)	2.471 (4)			
(μ-H)Ru$_3$(CO)$_8${μ_3-η^2-C≡C(*t*-Bu)}(Ph$_2$POEt)	1.315 (3)	1.947 (3)	2.207 (3)	2.268 (3)	25.5 (1)	39.8 (2)	36
			2.214 (3)	2.271 (3)			
Ru$_4$(CO)$_8${μ_2-η^2-C≡C(*t*-Bu)}{μ_3-η^2-C≡C(*t*-Bu)}(μ-PPh$_2$)-{Ph$_2$PC≡*t*-Bu)}	1.315 (9)	1.961 (7)	2.213 (7)	2.347 (9)	19.2 (2)	41.7 (4)	34
			2.178 (7)	2.202 (7)			
(c) μ_4-η^2							
Ru$_5$(CO)$_{13}$(μ_4-η^2-C≡CPh)(μ-PPh$_2$)	1.342 (11)	2.114 (8)	2.190	2.216 (8)	0	38.6 (4)	37
		2.095 (8)		2.163 (9)			
Ru$_4$Ni(CO)$_9${μ_4-η^2-C≡C(*i*-Pr)}$_2$(μ-PPh$_2$)	1.34 (3)	2.06 (2)	2.25 (2)	2.44 (3)			38
	1.38 (4)	2.31 (2)	2.28 (3)	2.50 (3)			
		2.04 (3)					
		2.27 (4)					
Ru$_5$(CO)$_{12}$(μ_4-η^2-C≡CPh)(μ-PPh$_2$)(μ_4-N$_2$CPh$_2$)	1.348 (18)	2.137 (13)	2.222 (12)	2.056 (13)		36.5 (7)	39
		2.180 (12)	2.052 (12)	2.438 (12)			
(d) μ_5-η^2							
Ru$_5$(CO)$_{14}$(μ_5-η^2-C≡CPh)(μ-PPh$_2$)	1.398 (13)	2.225 (8)	2.135 (8)	2.055 (8)		56.4 (4)	13c
		2.326 (8)	2.076 (9)	2.265 (8)			
Ru$_5$(CO)$_{12}$(μ_5-η^2-C≡CPh)(μ-PPh$_2$)(μ_3-η^2-PhC$_4$Ph)	1.340 (9)	2.106 (6)	2.336 (6)	2.204 (6)	0	48.4 (3)	1b
			2.299 (6)				
			2.292 (6)	2.212 (6)			

The simplest description of the bonding of the allenyl fragment in **4** is a σ-interaction between C(11) and Ru(2) and η-bonds to Ru(3) the C(10)–C(11) double bond and to Ru(1) from C(9)–C(10).

The overall features of **5** are strikingly similar to those of **4** with both the allenyl and phosphido ligands remaining virtually unperturbed. The only change in the framework is the replacement of C(3)–O(3) in **3b** with the methylene group across the Ru(1)–Ru(2) edge. The methylene bridge forms two strong but asymmetric Ru–C bonds of 2.108 (20) Å for Ru(1)–C(8) and 2.263 (21) Å for Ru(2)–C(8). Such asymmetry is not generally observed for μ-methylene ligands in homonuclear clusters[27] and may be due to the presence of different substituents trans to the methylene carbon atom. The Ru(1)–C(8)–Ru(2) angle of 81.6 (1)° is not atypical of values found for other methylene bridges having a metal–metal bond across the bridge. Compilations by Herrmann[27] have shown that these angles generally fall in the range 76–81° and are imposed by metal–metal bonding requirements. Compounds where no metal bond exists across the bridged edge generally have angles 30–40° greater.[27,28]

There is an alternative way of looking at the structures of **2a**, **3b**, **4**, and **5**, that is in terms of polyhedral skeletal electron pair theory (PSEPT).[29,30] For **3b** the three Ru atoms and the two carbon atoms of the acetylide occupy the vertices of an approximate trigonal bipyramid. Counting C$_\alpha$ of the acetylide as a two-electron donor as is appropriate for a skeletal (i.e. nonencapsulated) carbon atom and the C(*i*-Pr) group as a carbyne ligand, the PSEPT count for **3b** is 12 electrons or six pairs, appropriate for a closo five-vertex structure, as observed. Presumably the lone pair, formally on C(10), is partially delocalized into the multiple bond and the metal core. The 50-electron cluster **2a** has a quite different shape. The PSEPT count here is seven pairs leading to a nido structure based on an octahedron. In this case the missing vertex of the distorted octahedron is occupied by the phosphorus atom of the phosphido bridge, which is not of course bonded to Ru(2) and C(11). The atom C(10) again resembles the carbido carbon atom in an M$_4$ carbide with the "butterfly" comprising three ruthenium atoms and C(11).

---

(26) Gervasio, G.; Osella, D.; Valle, M. *Inorg. Chem.* **1976**, *15*, 1221.

(27) Herrmann, W. A. *Adv. Organomet. Chem.* **1982**, *20*, 160.

(28) See, for example: (a) Lin, Y. C.; Calabrese, J. C.; Wreford, S. S. *J. Am. Chem. Soc.* **1983**, *105*, 1679. (b) Morrison, E. D.; Geoffroy, G. L.; Rheingold, A.; Fultz, W. C. *Organometallics* **1985**, *4*, 1413. (c) McKeer, I. R.; Cowie, M. *Inorg. Chim. Acta* **1982**, *65*, L107. (d) Azam, K. A.; Frew, A. A.; Lloyd, B. R.; Manojlovic-Muir, L.; Muir, K. W.; Puddephatt, R. J. *J. Chem. Soc., Chem. Commun.* **1982**, 614. (e) Jandik, P.; Schubert, U.; Schmidbauer, H. *Angew. Chem., Int. Ed. Engl.* **1982**, *21*, 73.

(29) (a) Wade, K. *Adv. Inorg. Chem. Radiochem.* **1976**, *18*, 1. (b) Mason, R.; Thomas, K. M.; Mingos, D. M. P. *J. Am. Chem. Soc.* **1973**, *95*, 3802. (c) Evans, D. G.; Mingos, D. M. P. *Organometallics* **1983**, *2*, 435. (d) Mingos, D. M. P. *Acc. Chem. Res.* **1984**, *17*, 311.

(30) For a discussion of theoretical aspects pertinent to consideration of carbido and acetylide carbon atoms as skeletal framework atoms see: Halet, J. F.; Saillard, J. Y.; McGlinchey, M. J.; Jaouen, G. *Inorg. Chem.* **1985**, *24*, 1695.

Applying similar arguments to 4 but counting the CH_2 group of the allenyl unit as a ligand rather than a skeletal atom, Figure 3 immediately suggests a square-pyramidal core of three ruthenium and two carbon atoms. The PSEPT count of 14-electrons is consistent with this skeletal structure. The similarity of the CH_2 group bridging Ru(1) and C(10) to a μ-methylene bridge is apparent in Figure 4. Cluster **5** has the same skeletal framework as **4**, the only change being the replacement of a ligand CO by a μ-CH_2 unit.

The overall implications of the above PSEPT structural descriptions are clear. While C and CR fragments derived from acetylides or allenyl groups[31] appear structurally to function as vertices, CR_2 moieties of allenes are best thought of as bridging ligands. In chemical terms consideration of acetylide and allene carbon atoms as skeletal atoms in clusters suggests new approaches to the elaboration of these molecules, a topic which we are currently exploring.

^{31}P NMR Features of 2a, 2b, 3b, 4, 5, and 6. This series of clusters provides examples of molecules with μ-PPh_2 groups across open (no direct metal–metal interaction) and closed (short metal–metal bond) edges of a triangular M_3 skeleton. With precise X-ray data available (vide infra) for four compounds (**2a**, **3b**, **4**, and **5**) the series provides a nice test of the utility of $\delta(^{31}P)$ for probing structural changes in the frameworks of phosphido-bridged clusters. Compounds **2a** and **2b** are 50-electron clusters with two Ru–Ru bonds and μ-PPh_2 groups across the noninteracting metals (Ru(1)–Ru(3) = 3.466 (1) Å in **2a**). The ^{31}P shifts (**2a**, −73.6 ppm; **2b**, −73.3 ppm) are far upfield of the values in 48-electron **3b** (+334.9 ppm), **4** (+269.4 ppm), and **5** (+139.3 ppm) where the phosphido group bridges a short Ru–Ru distance (Ru(1)–Ru(3) = 2.8257 (4) Å in **3b**, 2.8252 (6) Å, in **4**, and 2.744 (2) Å in **5**). Thus the ^{31}P shift serves as a useful spectroscopic marker for opening and closing the triangular framework in these systems. These are also however significant differences between $\delta(^{31}P)$ values in **3b**, **4**, and **5** where the PPh_2-bridged Ru–Ru distances are bonding, and all three μ-PPh_2 groups are equatorial with respect to the Ru_3 planes. The comparison of **4** ($\delta(^{31}P)$ +269.4) and **5** ($\delta(^{31}P)$ +139.3) is particularly interesting since the structure of **5** is closely related to **4**, being derived from it by replacement of C(3)–O(3) with a μ-CH_2 group across the same Ru(1)–Ru(3) edge bridged by the PPh_2 ligand. Although the Ru(1)–Ru(3) distance in **5** is very short (2.744 (2) Å), it seems likely that the presence of a cis μ-methylene ligand is responsible for the high-field shift of $\delta(^{31}P)$ from **4** to **5**. Bridging methylene groups are thought to be electron-rich,[27] and their ^{13}C shifts reflect the accumulation of electron density at the alkylidene carbon atom.

Summary

Facile transformation of the acetylide in the phosphido-bridged cluster $Ru_3(CO)_9\{\mu_3\text{-}\eta^2\text{-}C{\equiv}C(i\text{-}Pr)\}(\mu\text{-}PPh_2)$ (**2a**) to an allenyl fragment in $Ru_3(CO)_8\{\mu_3\text{-}\eta^3\text{-}CH_2CC(i\text{-}Pr)\}(\mu\text{-}PPh_2)$ (**4**) has been accomplished via reaction with diazomethane. The allenyl cluster **4** is subsequently converted to the μ-methylene–allenyl compound $Ru_3(CO)_7\{\mu_3\text{-}\eta^3\text{-}CH_2CC(i\text{-}Pr)\}(\mu\text{-}CH_2)(\mu\text{-}PPh_2)$ (**5**) via transfer of a second methylene unit onto the cluster framework. Although the phosphido group does not participate in these novel transformations, it plays a key role in the chemistry in providing a reaction pathway for diazomethane addition. The conversion of "open" 50-electron **2a** to "closed" 48-electron $Ru_3(CO)_6(\mu\text{-}CO)_2\{\mu_3\text{-}\eta^2\text{-}C{\equiv}C(i\text{-}Pr)\}(\mu\text{-}PPh_2)$ (**3a**) via loss of CO and rapid reaction of the latter with CH_2N_2 are key steps in the reaction sequence. The ability of μ-PPh_2 bridges to "open" and "close" in this way to allow substrate additions while maintaining structural integrity should allow the development of new cluster moderated C–C bond forming processes.

Acknowledgment. We are grateful to the Natural Sciences and Engineering Research Council of Canada for financial support of this work in the form of operating grants (to A.J.C.) and scholarships (to S.A.M. and D.N.).

Registry No. **1a**, 77700-85-7; **1b**, 110511-62-1; **2a**, 77681-75-5; **2b**, 77700-86-8; **3b**·$0.5C_6H_6$, 110511-64-3; **4**, 87829-51-4; **5**, 87829-54-7; $Ru_3(CO)_{12}$, 15243-33-1; $PPh_2C{\equiv}C(i\text{-}Pr)$, 62199-59-1; $Ru_3(CO)_{10}\{PPh_2C{\equiv}C(i\text{-}Pr)\}_2$, 110511-63-2; $PPh_2C{\equiv}(t\text{-}Bu)$, 33730-51-7; diazomethane, 334-88-3; sodium benzophenone ketyl, 3463-17-0.

Supplementary Material Available: Complete listings of anisotropic thermal parameters (Tables S1–S4) and remaining bond lengths and angles (Tables S5–S8) for complexes **2a**, **3b**, **4**, and **5** (8 pages); listings of structure factors (Tables S9–S12) for complexes **2a**, **3b**, **4**, and **5** (72 pages). Ordering information is given on any current masthead page.

---

(31) Nucciarone, D.; Taylor, N. J.; Carty, A. J. *Organometallics* **1986**, *5*, 1179.

(32) MacLaughlin, S. A.; Taylor, N. J.; Carty, A. J., unpublished results.

(33) Carty, A. J.; Taylor, N. J.; Smith, W. F. *J. Chem. Soc., Chem. Commun.* **1979**, 750.

(34) Carty, A. J.; MacLaughlin, S. A.; Van Wagner, J.; Taylor, N. J. *Organometallics* **1982**, *1*, 1013.

(35) Ermer, S.; King, K.; Hardcastle, K. I.; Rosenberg, E.; Lanfredi, A. M. M.; Tiripicchio, A.; Tiripicchio Camellini, M. T. *Inorg. Chem.* **1983**, *22*, 1339.

(36) Carty, A. J.; MacLaughlin, S. A.; Taylor, N. J.; Sappa, E. *Inorg. Chem.* **1981**, *20*, 4437.

(37) Carty, A. J.; MacLaughlin, S. A.; Taylor, N. J. *J. Am. Chem. Soc.* **1981**, *103*, 2456.

(38) Lanfranchi, M.; Tiripicchio, A.; Sappa, E.; MacLaughlin, S. A.; Carty, A. J. *J. Chem. Soc., Chem. Commun.* **1982**, 538.

(39) Nucciarone, D.; Taylor, N. J.; Carty, A. J. *Organometallics* **1986**, *5*, 2565.